Professorship for Polymer Engineering

Polymer Mixing in a Single Screw Extruder

Part II: Mixing Quantification

University of Applied Sciences Windesheim

Colophon

Title: Polymer Mixing in a Single Screw Extruder (Part II: Mixing Quantification)

Publication number: LKT-DP-106741-2305

Publication date: September 2023

Authors: Dr. Ir. J. Buist
Dr. Ir. D.J. van Dijk
C. Hummel MSc
T.J. Mateboer MSc

Line of research:

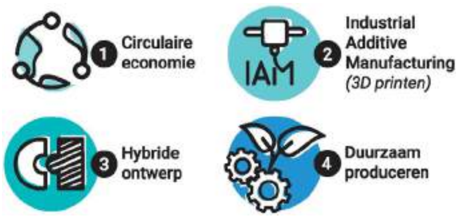

Funded by: TechForFuture

In collaboration with: Wavin T&I

The Professorship for Polymer Engineering of University of Applied Sciences Windesheim was founded in 2009; the group's objective is to improve the knowledge base on sustainable processing of plastics and composites within and through the higher education system. Its primary function is as a research group in Polymer Engineering, delivering output in the field of applied science. Befitting research groups at University of Applied Sciences, their research spans from TRL 4 to a maximum of 7: demonstration system prototype in an operational environment.

The team operates within market based projects and comprises lecturers from Civil Engineering, Industrial Product Design and Mechanical Engineering. The output of the projects is integrated into the curriculum of these study programs.

Contents

1 Introduction

This document is part of a series. This introduction contains a general preface for all documents and a specific outline of the subjects in this document.

1.1 General preface

The project 'Polymer Mixing in a Single Screw Extruder' is reported in a series of documents reporting the outcome of a four years research program, executed by the Professorship for Polymer Engineering of Windesheim University of Applied Sciences and Wavin Technology and Innovation department of the Orbia's community of companies. The project was funded by Centre of Expertise 'Tech For Future' in two successive projects, namely 'Sustainable extrusion processes in the production of pipes (TFF1703)' and 'Mixing in a single Screw extruder' (TFF1920).

Plastic pipes are commonly used for transport of fluids. The properties of the pipe depend (amongst others) on the plastic used in the production. The properties of the plastic in their turn, can be modified with additives. For example, the color of a pipe can be adjusted by the addition of a colorant to the polymer compound. The colorants are often mixed with the polymer using specialized equipment such as twin screw extruders. However, polymer (non-PVC) pipes are generally manufactured using a single screw extruder with a pre-compounded (pre-mixed) polymer. A basic single screw extruder has poor mixing characteristics. To improve mixing, different mixing elements with different mixing characteristics (like a spiral Maddock or a pin mixer) can be added after the compression zone of the extruder. Using a combination of these mixing elements, it could be more energy- and cost efficient to both mix and extrude with a single screw extruder.

The general objective of the program was to gain detailed knowledge of the extrusion process by modern analysis tools like computational fluid dynamics (CFD). A benefit of this tool could be a shorter development time of extrusion processes. To prove the strengths of these modern tools, the optimization and selection of mixing elements in single screw extrusion was chosen as these provide a challenging case.

Based on this general objective and the specified case, the following research questions were drafted:

1. What is a proper simulation method for polymer extrusion with respect to mixing?
2. How to quantify mixing quality in an extrusion simulation?
3. How to validate the simulation results and to validate the quantification of mixing?

The basis of the study is a literature search into mixing processes in extrusion, simulation of velocity, temperature, pressure and stresses in extrusion, quantification of mixing based on flow fields in extrusion and validation of mixing in extrusion experiments. Each document contains a specific part of this literature search, which is relevant for the subject in the respective document.

The first document *'Simulation Method':* Different simulation techniques, with respect to the discretization method and meshing method for the rotating screw, are analysed and demonstrated for different mixing elements. The selection of a suitable simulation method is not limited to single screw extrusion because in the future double screw extrusion might also be of interest. Preferably, a simulation method which is applicable for both single screw as well as double screw extrusion is selected.

The second document *'Mixing Quantification':* Several methods to quantify mixing quality were studied. In order to compare results, a method which is suitable for numerical simulations as for the experimental validation has to be selected.

The third document: *'Experimental Validation':* For the study described in this paper, a single screw extruder on lab scale, with multiple monitoring points in the barrel for temperature and pressure, was acquired. The screw of this extruder has a simple basic configuration with three zones and only one mixing element. Several screws with different mixing elements are available, to be able to make a clear distinction between the various effects. The screw is easy to exchange in the extruder barrel, which makes it possible to study different type of mixing elements. The barrel contains holes that can also be used to inject a second polymer or a colorant, for example between the compression zone and the mixing element.

Upon the completion of these research steps it should be possible to select a combination of mixing elements for an optimal mixing quality using numerical simulations.

1.2 Introduction into Mixing quantification

This report aims to seek out and develop methods to quantify mix quality for the comparison between extruder mixing sections. Ideally, the mix quality measure can be determined through both extrusion simulation and experiments.

The study began with a review of existing methodologies in literature, presented in section 2. Based on this review, several methods were chosen and further developed. Sections 3 through 5 describe these methods, their application guidelines, and their limitations.

The improved methods are then put to the test on four variations of a spiral Maddock mixing section. The process of implementing these methods and the resulting outcomes are shared in sections 6 and 7.

2 Literature study: mixing colorants with polymer in an extrusion process

Predicting mixing behavior of a single screw extruder using flow simulation is the goal of the overall sustainable extrusion project. This section contains the results of the literature search, which forms the base of this project. The study presents the current level of scientific knowledge of the relevant subjects but the goal is to answer the following question:

What methods are available to determine the mixing quality during extrusion experiments and extrusion simulations?

Polymer mixing can be done with either fluidic polymers or with solid polymers (granular mixing). This study focuses primarily on mixing of fluidic polymers. In this study a polymer is always a molten polymer unless stated otherwise.

2.1 Residence time distribution

The RTD (Residence Time Distribution) is the distribution of the residence time of materials inside a reactor for instance an extruder. It is often determined by the introduction of a number of particles into the extruder and measuring the residence time of each of those particles. If all particles travel a similar path then the RTD is narrow. If particles travel a wide variety of paths then a broad RTD is expected. With distributive mixing a large variety in particle paths can be expected. Therefore RTD is often used as a measure of distributive mixing [1-10].

In practical experiments a tracer is injected into the flow stream (usually at the hopper) in order to determine RTD. The tracer is injected during a time interval short enough to be viewed as a pulse. The concentration of tracer particles can be measured at specific locations inside the extruder or, more often, at the die exit. The methods to measure the tracer concentration can be based on a number of principles [11]:

- Radioactivity with MnO_2, La_2O_3
- Ultrasound reflectivity with fillers such as carbon black
- Electrical conductivity with KNO_3, $NaNO_3$, KCl
- Light reflectivity with TiO_2
- Light transmission with carbon black
- Light emission (fluorescence) with anthracene
- Mass fraction of a mica tracer after thermal decomposition of the polymer

Zhang *et al.* developed a RTD measurement system, with fluorescent light and optical sensors, capable of measuring the tracer concentration at several locations inside the extruder barrel [3]. RTD in several twin screw extruder setups was measured and compared in order to determine the extruder setup with the best mixing quality, see Figure 1.

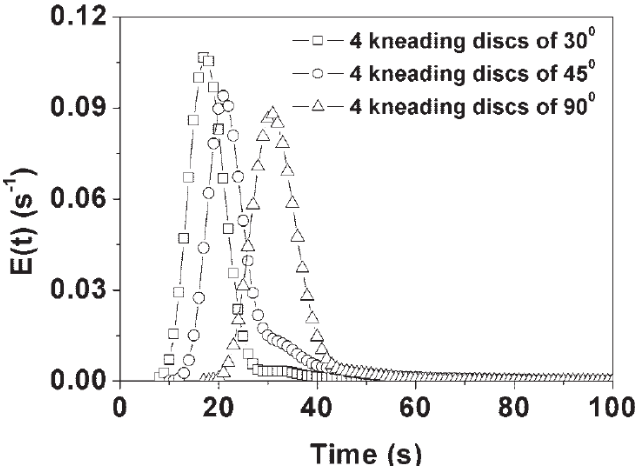

Figure 1. RTD: Tracer concentration per time interval as a function of time. A variety of kneading discs were used in 3 different twin screw extruder setups. The setup with kneading discs of 90° shows the broadest distribution therefore has the most distributive mixing of all 3 setups. (Figure copied from figure 11, reference [3]).

RTD can also be determined in an extrusion simulation by particle tracking. Zong *et al.* found agreement between simulated and measured RTD in a twin screw extruder, see Figure 2 [6].

In this experiment a mica powder was added in pulses into the feeder. Extrusion samples were collected every 10s. After high-temperature calcination, the mass fraction of mica powder was measured to determine RDT.

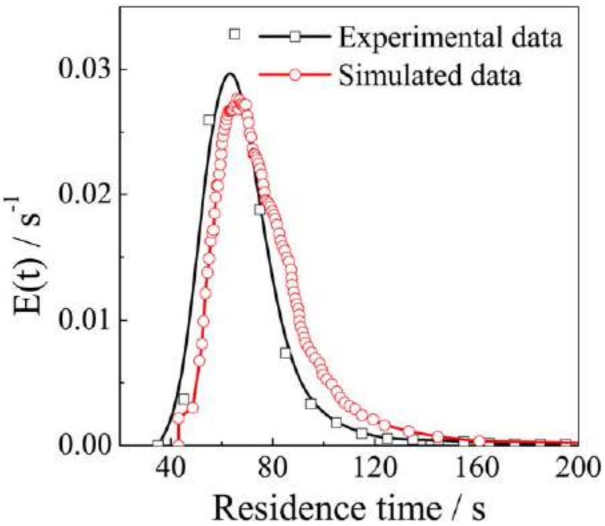

Figure 2. Simulated and experimental found RTD of a twin screw extruder. (Figure copied from figure 5 of reference [6]).

In summary, there are several methods available to determine the RTD with experiments, the RTD can also be determined in simulations. These simulation results can be verified through RTD experiments.

2.2 Shannon entropy

Shannon introduced the Shannon entropy or information entropy (*S*) to quantify the amount of data produced by a data source [2, 8, 12-22]. A theoretical explanation of Shannon entropy is given in chapter 3.1. In this paragraph the use of Shannon entropy on the mixing efficiency of extrusion processes will be discussed.

Alemaskin *et al.* studied single screw mixing of two ABS melts with simulations and experiments [12, 16-22]. Yellow and blue ABS compounds were used. The ABS pellets were premixed in a 20/1 ratio of yellow/blue color. Mixing quality was determined with the Shannon entropy. When the steady state operation phase of the extrusion experiment was reached, the screw was stopped and the barrel was rapidly cooled to room temperature. Then, the screw was removed from the barrel and the polymer solidified in the screw channel was evaluated. 7 samples were taken at several positions inside the extruder. A photograph was made of each sample, see Figure 3.

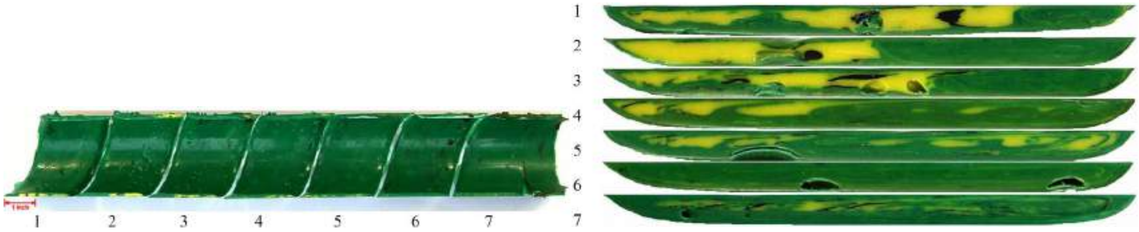

Figure 3. Slices of samples from inside the extruder. Left: the ABS mixture as found in the extruder with numbers at each sampling position. The flow direction is from left to right, a higher sample number corresponds to a greater distance traveled through the extruder. Right: samples 1 to 7. (Figure copied from figure 5.3 and 5.4, reference [21]).

The samples showed yellow and green material, green was interpreted as a mixture of the yellow and blue ABS. The yellow areas were interpreted as un-mixed yellow ABS. The pictures also showed some air pockets inside the extruder. The influence of these air pockets, on the mix quality, was estimated to be minimal. The images of the samples were used to qualitatively determine an increase in mixing quality as a function of distance traveled through the extruder. A quantitative measure of distributive mixing quality was determined with the relative Shannon entropy. The relative Shannon entropy is in this particular case, a measure of image color homogeneity. Each picture, of the samples, was converted into monochromatic images with a specific color (red, green or blue). The photographs of the samples were divided into equally spaced bins. A graph of the relative Shannon entropy was made of each sample based on color. The Shannon entropy was determined at several scales of observation from 10 bins up to 54000 bins. Figure 4 shows the monochromatized images of the samples and the relative Shannon entropy of each sample.

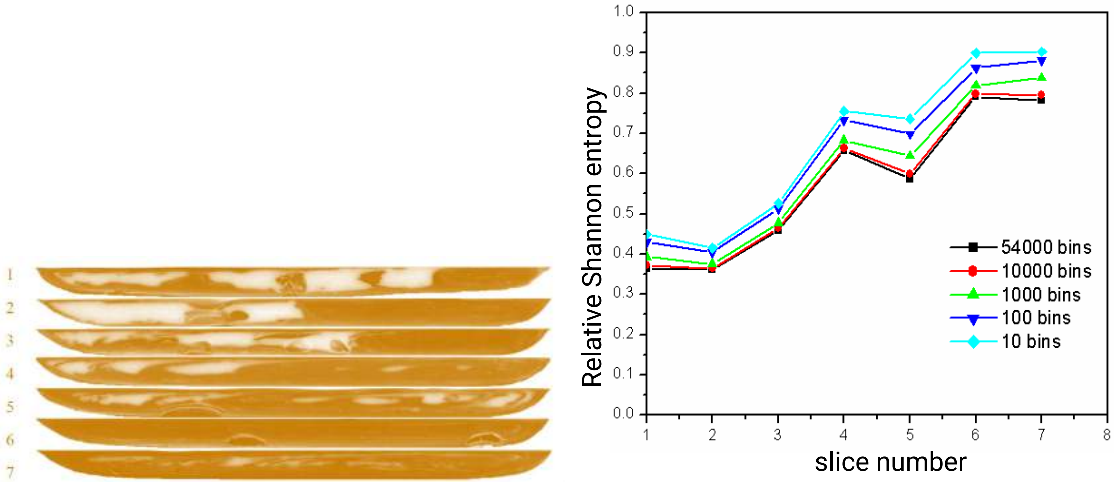

Figure 4. Left: the same slices of samples as shown in Figure 3, with only the red color of the image shown. Right: Relative Shannon entropy of the red monochromatized slices. The slice number relate to the distance traveled in the extruder, see Figure 3. (Figure copied from figure 5.6 and 5.10, reference [21]).

The relative Shannon entropy of the red monochromatized image shows an increase with increasing distance traveled through the extruder. In other words, the mixing quality increased with distance traveled through the extruder. The relative Shannon entropy can be seen to decrease with an increased number of bins. This shows that mixing quality appears to be high at a macroscopic level while the mixing quality is relatively less at a smaller scale of observation.

The single screw extrusion process was also simulated by Alemaskin *et al.* A single phase model was applied, which is allowed since both fluids were described with the same rheological properties and the fluids were chosen to be miscible. The simulations were performed with Fluent. The pressure inside the barrel, which was determined experimentally, was used as a boundary condition for the simulation. The simulations and experiments showed agreement in the flow rate.

20000 yellow and 1000 blue particles were introduced in the simulation. The initial position of the tracer particles in the simulation were chosen to be similar to a sample image of the experiment. This initial position is with a very low mix quality, the yellow ABS is on one side and the green ABS on the other. Both the experimental sample and the initial position of the particles are shown in Figure 5.

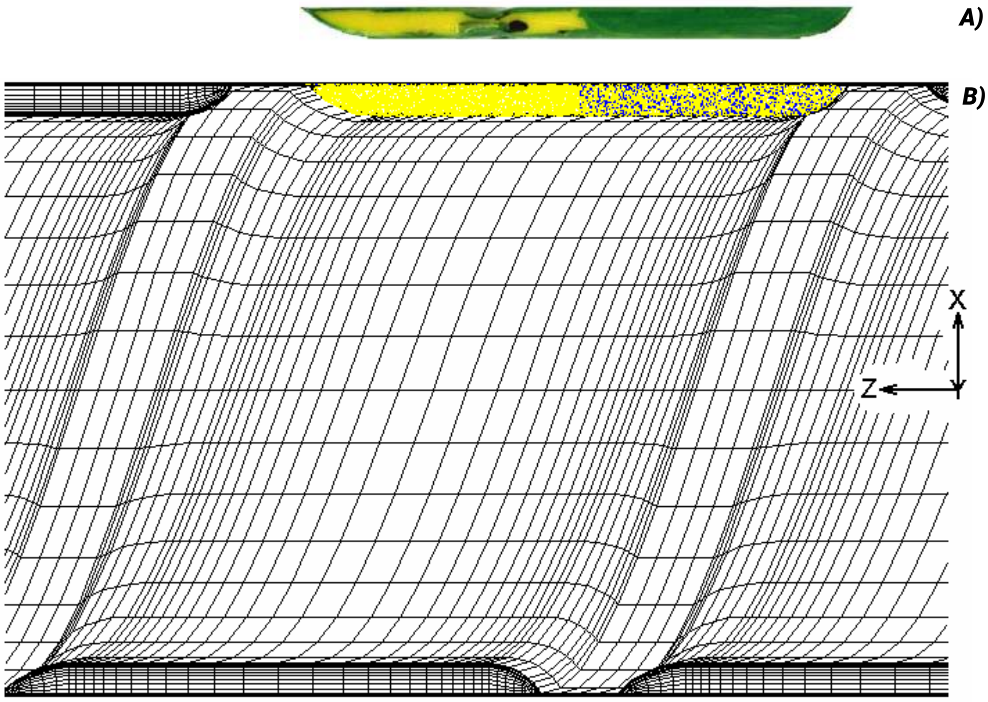

Figure 5. Depiction of ABS mixture inside the extruder. The experiment at the top and simulation below. (Figure copied from figures 6.1, 6.3 and 6.4 reference [21]). A) Sample from experiment. B) Simulation with tracer particles (blue) introduced at positions corresponding to the experiment

Sample slices were made of the simulations similar to the images from the experiments. The positions of the sample slices in the simulations correspond with the position of the experimentally acquired samples. The position of the tracer particles were determined in each simulation sample.

Figure 6. Comparison between sample images of the extruder experiments and the slices of the simulated extruder with the tracer particles. The upper images correspond to a short distance inside the extruder, the lower images correspond to positions further down the extruder. (Figure copied from figure 6.7, reference [21]).

As can be expected, both the simulations and the experimental data show an increase in mixing quality qualitatively at a larger distance traveled inside the extruder. But according to Alemaskin *et al.* the experimentally obtained images show more complex mixing features compared to the numerical results. The Relative Shannon entropy was calculated for each simulated slice.

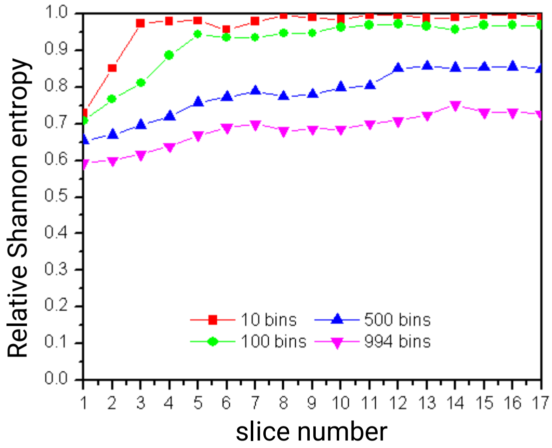

Figure 7. Relative Shannon entropy of simulated yellow and blue tracer particles. The slice number is in the order of distance traveled inside the extruder, see Figure 3. (Figure copied from figure 6.8 of reference [21]).

The relative Shannon entropy was found to increase with increased distance traveled through the extruder in the simulations. The increased Shannon entropy corresponds with increased mixing quality. This increase in relative Shannon entropy was determined for both the experiments as well as the simulations. Relative Shannon entropy is quite high early on in the simulated extruder for a small number of bins, while the entropy is still quite low for a high number of bins. This again confirms that although mixing quality appears to be high at a macroscopic level (small number of bins), the mixing quality is still low at a smaller scale of observation. The difference in relative entropy as a function of number of bins seems to be higher with the simulations compared to the experiments. In this particular study Alemaskin *et al.* did not compare the relative Shannon entropy of the simulations with the experiments. It is not clear whether the method of determining relative Shannon entropy was not appropriate for quantitative comparison between the simulations and experiments. The relative Shannon entropy of the simulations and experiments do not seem to be in agreement although a direct comparison is difficult since sample slice numbering scheme differs between simulation and experiment.

Alemaskin *et al.* determined the Shannon entropy of samples inside the extruder but this method could also be applied to extrudate samples, which are more easily obtained. The mix quality in the extrudate samples is the result of mixing in the whole extruder, including the screw zones, the mixing zone and the die. Consequently, extrudate samples cannot provide detailed information of mixing in specific sections (such as the mixing zone of the screw). While samples from inside the mixer can provide information what the mix quality is in each extruder section.

2.3 (Optical) radiation reflection, transmission and absorption techniques

Several methods exist to determine the mixing quality using radiation. Radiation includes optical light and the methods can be categorized into radiation reflection, transmission and absorption. This section discusses several techniques to determine mixing quality with radiation.

2.3.1 Radiation reflection

Visible streaks, swirling and blotches in the extrudate are all signs of poor distributive mixing quality [23]. With an optical microscope the *distributive* mixing quality can be determined on a smaller scale than by eye. A drawback of such small scale observations is that the images might not be representative of the whole mixture. Optical microscopes can also be used to determine *dispersive* mixing quality [24]. Yamada *et al.* performed extrusion simulations and experiments using polypropylene with a $CaCO_3$ filler [25]. Several extruder configurations were used in the experiments. A reflected light optical microscope was used to determine the amount of dispersive mixing of the $CaCO_3$. $CaCO_3$ agglomerates of more than 100 μm^2 could be observed, see Figure 8.

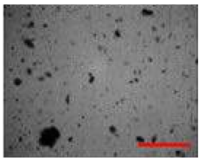

Figure 8. Reflected light optical microscope images of $CaCO_3$ agglomerates in polypropylene. The black spots are the $CaCO_3$ agglomerates. (Figure copied from figure 7 of reference [25]).

The number of $CaCO_3$ agglomerates per unit of observed area was determined from multiple microscopic images. This procedure was used for each extruder configuration allowing a quantitative comparison between the different screw configurations.

Hopmann *et al.* studied the dispersive mixing of carbon black in rubber in an extruder with a similar method [26]. A MonTech Disper Tester 3000 was used for dispersive mixing analyses. The Disper Tester is an instrument with an optical reflective microscope capable of measuring the area occupied by carbon black agglomerates [27].

Similar results to reflected light optical microscopy were obtained by scanning electron microscopy (SEM) [24]. SEM gives a much higher resolution (nm) compared to optical microscopy (µm). A disadvantage is the extremely small area of observation which can lead to misleading statistical results unless a large number of images are taken and evaluated.

2.3.2 Radiation transmission

Transmitted light techniques can also be used to determine dispersive mixing quality [24]. This technique requires thin slices of the mixture, thin enough to let light pass through. The dispersive mixing quality can be determined by counting the number of agglomerates per unit of volume.

A similar procedure and results can be obtained with transmission electron microscopy (TEM) [24]. With TEM very small (0.2 nm) agglomerates can be observed. A disadvantage is the small area of observation, similar to SEM. Sample preparation for transmitted techniques can be difficult, especially when working with very thin (100 nm) sample slices.

Micro-radiography is another technique that can be used to study dispersion [24] and is very similar to optical transmitted light techniques. This method is only applicable when there is a high difference in radiation absorption between the colorant and the polymer. Therefore, this method is suitable to study polymer mixing with inorganic colorants but less suitable to study mixing with organic colorants (such as carbon black). An advantage of micro-radiography is however the relatively thick specimens that can be used.

Dispersive mixing quality of mixing equipment can also be determined without counting the number of agglomerates but by measuring the total light absorption of a sample [28]. This method is based on more light absorption at larger total particle surface area when pigment is well dispersed. A spherical particle has a higher surface to volume ratio when it is smaller. If light absorption is mostly a phenomenon at or near the surface, than more light will be absorbed if the surface area increases. Therefore a higher ratio of surface area to volume will result in more light absorption per unit of volume. Smaller light absorbing particles (such as single carbon black particles) will absorb more light compared to large particles with the same total volume. Carbon black agglomerates can be viewed as relatively large light absorbing particles. Therefore the light absorption of a mixture increases with increased dispersive mixing, which in turn means that a mixture with fewer or smaller carbon black agglomerates will have a higher light absorption compared to a mixture with larger agglomerates at the same total carbon black volume.

Because some light transmission is necessary for this method, it is only applicable to thin samples and not suitable for high filler loadings and therefore it is not often applied in mixing studies. Accurate mixing quality measurements do not seem likely with this method.

2.4 Ultrasonic reflection

Within a mixture, the dispersed material often has different acoustic properties compared to the matrix material. This results in an echo from the dispersed phase or solid particles when a sonic pulse is emitted into a fluidic mixture. Particle or dispersed phase concentration can be determined with the help of echo location [29], which is effectively a measure of distributive mixing. Ultrasonic Doppler velocimetry (UDV) is a method to determine the velocity profile of a solution [30]. An ultrasonic pulse is emitted by a transducer, the same transducer receives the echo from tracer particles suspended in the fluid. The position of the particles is obtained from the time lapse between pulse emission and echo reception. The velocity of the particles is obtained from the Doppler frequency shift from the echo. UDV is applied to determine the velocity profile of a polymer melt flow [30-34]. Putz *et al.* developed a UDV with transducer integrated in an extruder die capable of functioning at temperatures up to 250° C [32, 33]. Ein-Mozaffari and Upreti used UDV to verify the velocity profile of a shear thinning fluid as calculated with CFD (a water xanthan gum solution) [35].

Chemloul *et al.* used UDV to determine velocity profiles of a starch water solution flow between two plates [29]. Glass beads were mixed through the solution. The echo of the UDV pulses were also used to determine glass beads concentration profiles, see Figure 9.

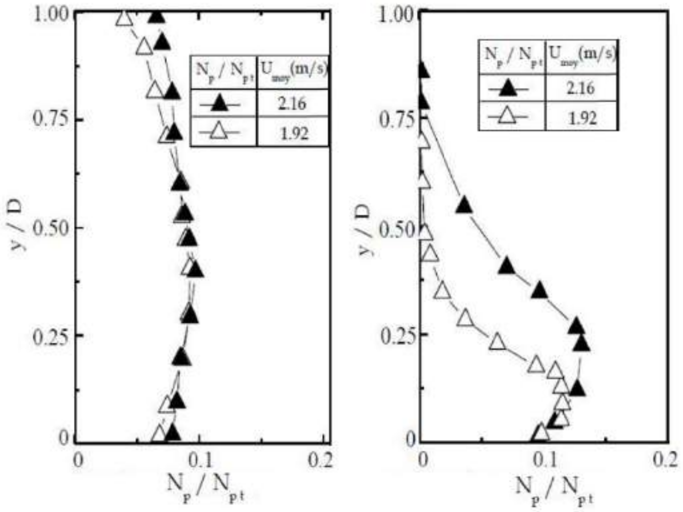

Figure 9. Concentration profile of glass beads in a water starch solution in a flow between two plates as a function of height between the two plates. Measurements were performed at two flow rates, see legend. Left: smaller glass beads of 0.13 mm. Right: larger glass beads of 0.40 mm. (Figure copied from figure 7, reference [29]).

2.5 Other properties as a measure of mixing quality

Several material properties depend on the mixing quality. These include electrical properties and surface roughness and are proposed as a measure of mixing quality in some studies although it is questionable how feasible and accurate they are. The next section focuses on these mixing quality dependent properties and methods to determine mixing quality.

2.5.1 Electrical properties

An increase in dispersive mixing results in a reduction of electrical resistivity of a fluid-solid mixture containing a conductive solid additive. Usachev *et al.* continuously measured the resistivity of a mixture during mixing [24]. The resistance decreased until it reached a stable low value. This method is dependent on conductive additive volume fraction and particle size. Therefore resistivity alone is not sufficient to determine the degree of dispersion.

2.5.2 Surface roughness

Surface roughness and carbon black agglomerate size were correlated in a freshly cut rubber sample [24]. Carbon black agglomerates deflect the cut path due to their relative hardness and therefore the surface roughness can be used as an indication for dispersive mixing quality. The DisperGRADER Alpha View (Alpha Technologies) is a device that evaluates the quality of dispersion by quantifying the surface roughness of a freshly cut specimen using an optical microscope in the reflection mode [36]. This method was developed specifically for rubber mixtures. It is not clear how feasible it is to apply this method to other polymer mixtures.

2.6 Conclusion: literature search

This literature study is focused on the quantification of polymer mixing experiments using an extruder and CFD mixing simulations of an extruder.

Several studies focused on the parameters available to determine the mixing quality of extrusion experiments or extrusion simulation. Particle tracking was often applied to simulations. Residence time distribution and the Shannon entropy as determined with particle tracking were shown to be measures of distributive mixing quality. For extrusion mixing experiments several methods are available to determine the mixing quality. The *distributive* mixing quality can be found with residence time distribution and the Shannon entropy. *Dispersive* mixing can be determined with (optical) radiation techniques which often involve counting the number of dispersed units. These methods can be applied to the extrudate or to the mixture inside the extruder barrel. Extrudate samples are more easily obtained compared to samples from inside the extruder, but these samples naturally hold less information of the mixing process inside the extruder. Other methods to determine the mixing quality were found, based on ultrasonic reflection, electronic properties and surface roughness but these generally lack accuracy or ease of implementation.

Some studies compared simulation and experiment. Zong *et al* studied mixing and found agreement in the residence time distribution of experiments and simulations. For most other studies the comparison between simulation and experiments is qualitative and not quantitative. Some studies also compared simulation and experiments based on parameters that are not linked to mixing quality, like pressure. In these particular cases they verified the simulations without verifying the mixing itself.

2.7 Recommendations: literature search

Several methods to determine the mixing quality are available. It is preferable to acquire a significant amount of information from the mixing process for comparison between experiments and simulations. And to use the same quantity for expressing mix quality in both experiments and simulations.

Shannon entropy is recommended since it can be used to express mix quality in a cross section of the extruder in both experiments and simulations.

Furthermore, it is recommended to use the RTD to determine mix quality, in the extrusion direction, in both simulations and experiments.

3 General methods and guidelines for Shannon entropy calculations to quantify distributive mixing

This section presents the tools developed to quantify distributive mixing in single screw extruder simulations using Shannon entropy, along with outlining the requirements and limitations when applying these tools.

Tools in Ansys and GNU Octave were applied or developed to determine distributive mixing quality with Shannon entropy calculations. Details about the Shannon entropy calculation using tracer particles can be found in sections paragraphs 3.1 and 3.2. The limitations of the Shannon entropy as a measure for distributive mixing quality when the particle inflow section is larger than a single outflow bin are presented in paragraph 3.3.

Paragraph 3.4 discusses the use of a specific bin distribution scheme for determining mixing quality in specific directions.

A low number of tracer particles may result in random and systematic errors in the Shannon entropy, guidelines for a minimum number of particles and uncertainty calculations are given in paragraph 3.5.

Application of these methods in simulations for comparison between simulations is detailed in paragraphs 3.6 and 3.7.

3.1 Shannon entropy

Shannon introduced the Shannon entropy or information entropy (S) to quantify the amount of data produced by a data source [2, 8, 12-22]. Shannon entropy is sometimes used as a statistical measure of mixing. A mixture is geometrically divided into a number of bins (M) of equal size to determine the Shannon entropy.

$$S = -\sum_{i=1}^{M} p_i \ln p_i \qquad 1$$

p_i is the probability that a tracer, selected at random, will lie in bin i. p_i is equal to the number of tracers (c_i) in bin i divided by the total number of tracers (N). Note that the probability is determined by the fraction of particles contained within a particular bin.

$$p_i = \frac{c_i}{N} \qquad 2$$

Maximum Shannon entropy is reached if particle concentrations are equal in all bins. In other words, if particles are evenly distributed (high distributive mixing), the maximum Shannon entropy is reached. The maximum value of Shannon entropy is ln(M). Relative Shannon entropy (S_{rel}) can be used to compare Shannon entropy with different numbers of bins.

$$S_{rel} = \frac{S}{\ln(M)} \qquad 3$$

Shannon entropy is a single value rating of a probability distribution. Figure 10 illustrates the relation of a probability distribution and the relative Shannon entropy.

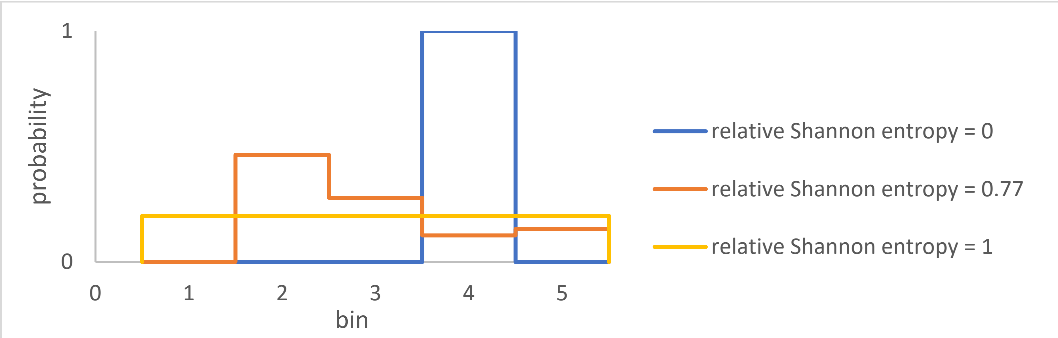

Figure 10. Three hypothetical examples of a probability distribution as a function of bin number and the corresponding relative Shannon entropy.

A low value of S_{rel} corresponds to a low mixing quality, maximum entropy is reached when $S_{rel} = 1$, as is illustrated in Figure 10. Relative Shannon entropy lies in the range $0 < S_{rel} \leq 1$. This well-defined range facilitates an intuitive estimation of the mixing quality.

The bin size determines the scale of observation. Mixing quality at a macroscopic level can be determined with a small number of bins. Mixing quality on a microscopic level needs to be determined with a high number of bins. Therefore, M is an important parameter in the description of distributive mixing quality.

3.2 Theoretical application to a cylindrical mixer with a circular inflow and outflow

To determine the Shannon entropy a single screw extruder can be viewed as a cylinder. The exact screw shape is not relevant for this method to determine the Shannon entropy.

Figure 11. Schematic representation of a single screw extruder. Left: extruder viewed as a cylinder. Right: inflow and outflow of the extruder.

Mixing can be illustrated by introducing tracer particles at the inflow of the cylindrical extruder and observing where they flow out.

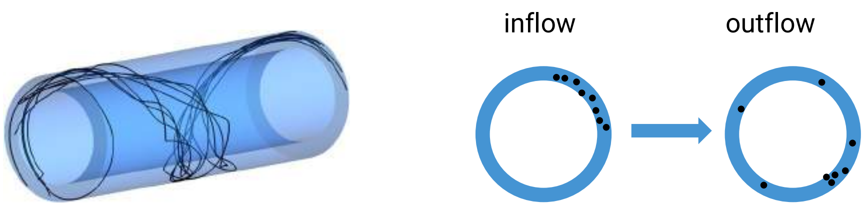

Figure 12. Tracer particles are introduced in the cylindrical extruder.

Distributive mixing quality can be calculated by dividing the outflow into bins, followed by a calculation of the Shannon entropy with the probability that a particle path goes through the bin. Several systematic division schemes can be applied. Some examples are shown in Figure 13.

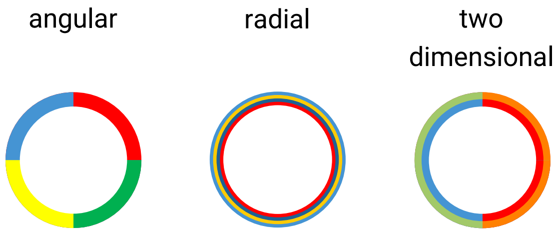

Figure 13. Outflow divided into four bins. Left: angular division, middle: radial division, right: two dimensional (radial and angular).

The setup with angular bins is discussed here, but the methodology can also be applied onto other bin schemes. The relation between bin distribution scheme and mix quality is discussed in more detail in section 3.4. Figure 14 shows three examples of an outflow with four bins and eight tracer particles.

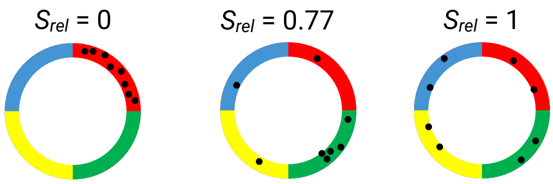

Figure 14. Outflow divided into four radial bins with eight tracer particles. Left low quality mix (S_{rel} = 0), middle: higher quality mix (S_{rel} = 0.77), right: high quality mix (S_{rel} = 1).

Shannon entropy is a measure of the quality of mixing in a certain area, but it does not quantify the mixing quality of the extruder screw. For example, if the tracer particles are distributed equally across the inflow, then the particles will be distributed very well across the different bins at the outflow. This results in a high Shannon entropy (suggesting high mixing quality) regardless of the mixing properties of the extruder. Therefore, it is recommended to have a particle distribution at the inflow of S_{rel} = 0. This can be achieved by introducing the particles in a section of the inflow with equal size and shape as a single outflow bin.

3.3 Introducing tracer particles in a larger section at the inflow

The bin size determines the scale of observation, as discussed in paragraph 3.1. One might want to determine the distributive mixing at both macroscopic and microscopic levels. This can be achieved by calculating the Shannon entropy with both a small number and a large number of bins. Paragraph 3.2 recommends a tracer particle inflow section of the same size as a single outflow bin. It might seem efficient to deviate from this recommendation by only using a single particle inflow section for all the Shannon entropy calculations with the different bins sizes. But using an inflow section larger than a single outflow bin will result in a higher Shannon entropy than is in agreement with the distributive mixing quality. Up to $S_{rel\,=}$ 1 (high distributive mixing quality) can be found even when there is no mixing in the extruder.

This paragraph discusses how a larger particle inflow section results in disagreement between the Shannon entropy and distributive mixing quality. This is illustrated using a model extruder that does not mix at all. It is important to note that the equations in this paragraph are only applicable to this specific example. But the conclusion that a particle inflow section larger than a single outflow bin might result in an erroneously high Shannon entropy is applicable to all calculations in accordance to paragraph 3.1.

In this example the tracer particles have the same angular position at the outflow as they had at the inflow, see Figure 15. This means a very low mixing quality. Shannon entropy calculations will also show a low mixing quality ($S_{rel} \approx 0$) if the tracer particle inflow section is the same size as a single outflow bin. But in this example the particle inflow section is a multiple of a single outflow bin.

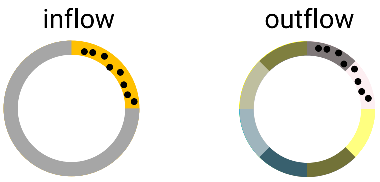

Figure 15. Inflow and outflow of an extruder without mixing. Introducing tracer particles at the inflow in a section that is a multiple of a single outflow bin.

Some of the outflow bins are occupied by some particles, the number of occupied bins (*a*) are a subset of the total number of outflow bins (*M*). For this example, the particles are equally divided over the occupied bins. In this case, the probability (p_a) of a particle to flow into an occupied bin is calculated with equation 4. While the probability is zero in the bins without particles.

$$p_a = \frac{1}{a} \qquad (4)$$

Equation 4 can be applied to the example illustrated in Figure 15. The tracer particles all end up into two bins (a = 2), therefore probability of these two bins: p_a = 1/2. The probability of the other 6 bins: p = 0.

Equations 1 and 3 reduce to:

$$S_{rel} = \frac{-a \cdot p_a \ln p_a}{\ln M} \qquad (5)$$

$$S_{rel} = \frac{-\ln\left(\frac{1}{a}\right)}{\ln M} \qquad (6)$$

The number of occupied outflow bins (*a*) can be expressed with a ratio (*q*) of the total number of outflow bins (*M*).

$$a = q \cdot M \qquad (7)$$

Combining equations 6 and 7 results in:

$$S_{rel} = \frac{-\ln\left(\frac{1}{q \cdot M}\right)}{\ln M} \qquad (8)$$

$$S_{rel} = \frac{-\ln\left(\frac{1}{q}\right)}{\ln M} + \frac{\ln M}{\ln M} \qquad (9)$$

In this example the Shannon entropy increases with an increase in the number of bins (*M*), see Figure 16.

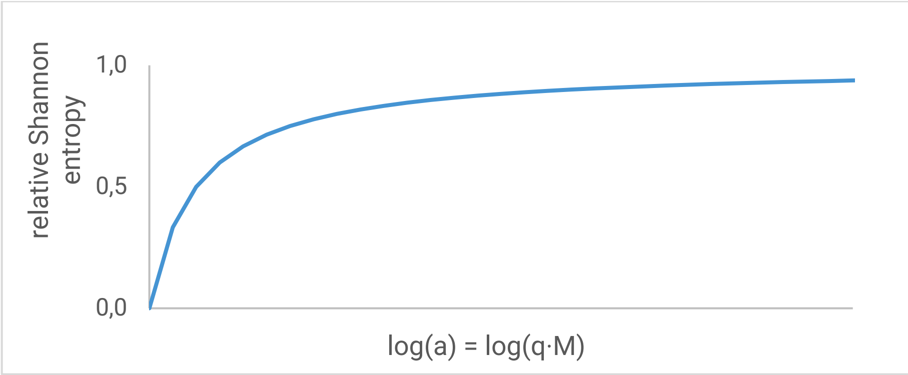

Figure 16. Relative Shannon entropy as a function of the number of occupied bins (a) calculated with equation 9.

The right side of equation 9 consists of two parts, ln(M)/ln(M) = 1 and -ln(1/q)/ln(M). This second part reduces to zero if M>>q. The relative Shannon entropy increases to one when the number of bins increases to M>>q.

$$S_{rel}\left(q \ll M\right) \approx 1 \qquad (10)$$

Crucially, the $S_{rel} \approx 1$ contradicts the reality of very low mixing quality, given that the extruder performed no mixing whatsoever. This inflated Shannon entropy is a consequence of the particle inflow section being significantly larger than the Shannon entropy bin.

In practice $S_{rel} \approx 1$ might not be approached due to practical limitations in the number of bins. But the increase in S_{rel} is not negligible even when the particle inflow section is moderately larger than a single outflow bin. For example, if the particle inflow section is twice the size of a single outflow bin (a = 2) then S_{rel} = 0.3 for M = 10 and S_{rel} = 0.1 for M = 1000. These Shannon entropies are significantly higher than the Shannon entropy ($S_{rel} \approx 0$) expected for a low mixing quality. Therefore, it is recommended to introduce tracer particles into a section of the same size as a single outflow bin.

3.4 Bin distribution scheme

The outflow of an extruder is divided into several bins for Shannon entropy calculations. Several systematic division schemes can be applied. Some guidelines and considerations for choosing a bin division scheme are given in this section.

3.4.1 Different bin distribution schemes and Shannon entropy calculations

Three bin distribution examples are shown in Figure 13 and Figure 17.

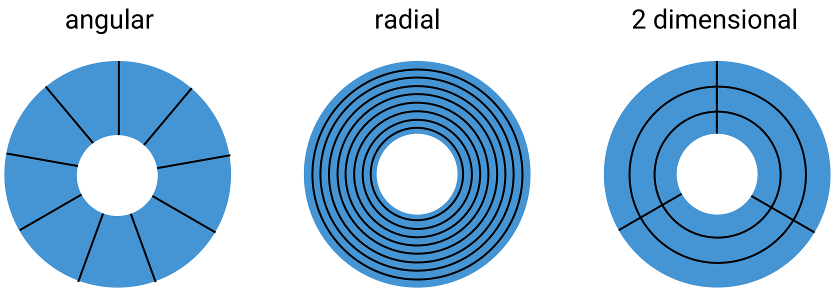

Figure 17. Outflow divided into nine bins. Left: angular division, middle: radial division, right: two dimensional (radial and angular).

Each bin division scheme demonstrates different aspects of distributive mixing, i.e. distributive mixing in the angular, radial direction or both. Each of the three examples consists of 9 bins. In their respective dimensions, both the radial and angular bins are smaller than the bins in the 2-dimensional distribution. Therefore fewer particles are needed for the same scale of observation with the angular and radial bin schemes compared to the 2 dimensional bin scheme. The same number of bins allows for a smaller scale of observation with the one-dimensional schemes (angular and radial bin schemes) compared to the 2 dimensional bin scheme.

Radial direction and angular direction are two different dimensions. But a 2-dimensional bin division scheme might represent a different aspect of the distributive mixing than the angular Shannon entropy and radial Shannon entropy combined. This is illustrated with an example in Figure 18 showing distributive mixing in two steps: first in radial direction and then in angular direction.

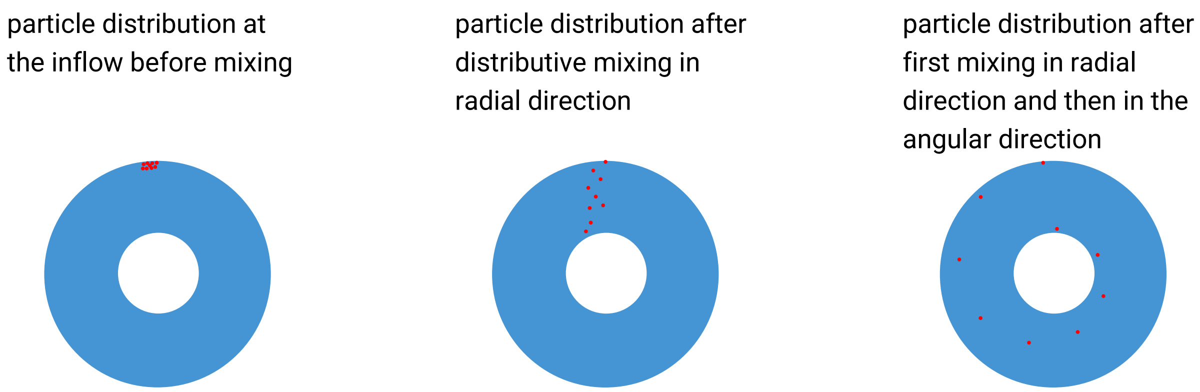

Figure 18. Distributive mixing in two steps, first in radial direction (middle), and then in angular direction (right).

The result of both mixing steps is a spiral distribution of particles. The Shannon entropy is calculated for the angular, radial and 2-dimensional bin distribution, see Figure 19.

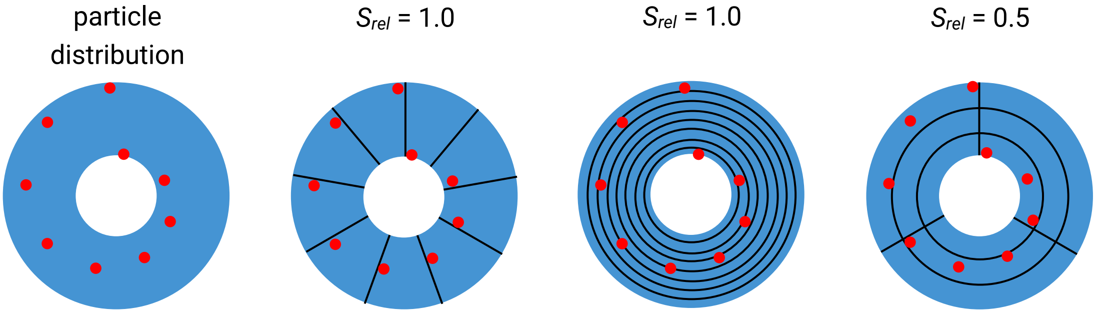

Figure 19. Particle distribution at the outflow. From left to right: outflow without bins, angular bin distribution, radial bin distribution, 2 dimensional bin distribution.

S_{rel} = 1 is calculated for both the angular and radial bin distributions. This suggest good mixing in both dimensions (angular, radial), but the mixing is not good according to the calculations with the 2 dimensional bin distribution (S_{rel} = 0.5). This shows that angular and radial Shannon entropy do not hold the same information as a 2-dimensional Shannon entropy, and the 2-dimensional Shannon entropy cannot be derived from the angular and radial Shannon entropy.

In conclusion, there is not one specific bin distribution scheme optimal for all applications, It varies depending on the specific requirements of the mix. For instance, to achieve visually pleasing coloring for a product, both opaque coloring and uniform distribution across the surface are necessary. Consider a thin product such as a large-radius pipe made of a semi-translucent polymer: uniform distribution of the colorant across the surface is crucial for visual appeal, while its distribution over the thickness might be less important as long as it maintains opaqueness. Given that the pipe surface aligns with the angular direction, a high mix quality in the angular direction is relevant. This mix quality can be more effectively determined using an angular bin distribution scheme. However, for different extrusion profiles, alternative bin application schemes with varying numbers of angular and radial bins may be required.

3.4.2 Bin size distribution in relation to flow rate distribution

An extrusion product with a high mix quality is a product where the additive is homogeneously distributed over the mass of the extrusion product. While in this study an extrusion process is considered with tracer particles, without a specific mass, but with a specific mass per unit of time (flow rate). Consequently, in extrusion simulation the mix quality is how homogeneously the tracer particles are distributed over the flow rate. Therefore, the flow rate in each bin should be equal.

Shannon entropy is both a function of mix quality and flow rate distribution

If the flow rate in the bins is not equal, then the Shannon entropy is a function of both mix quality and flow rate distribution and is not unequivocally a measure of mix quality.

For example, consider a high quality distributive mix with the particles equally distributed through the fluid, in this case a high Shannon entropy is expected. The number of particles per bin should be equal in order to reach a high Shannon entropy. But if more fluid flows through one bin than through the other bins, then the number of particles flowing through that one bin will also be higher. This results in a lower Shannon entropy, falsely suggesting a low mixing quality. The low Shannon entropy is in contrast with the high mixing quality and is an error due to uneven distribution of flow rate through the bins.

Quantify the flow rate distribution in the bins

Therefore, it is recommended to check whether the flow rate distribution is homogeneous in the bins. The flow rate distribution across the bins can be quantified with the Shannon entropy for flow rate (S_Q). S_Q is a measure of flow rate distribution, not a measure of mixing quality. The flow rate distribution is equal if $S_Q \approx 1$.

The same bins should be used for distributive mixing as for Shannon entropy calculations. The probability (p_{Q_i}) that a unit of fluid travels through bin *i* can be expressed as a function of flow rate through the spiral Maddock ($Q_{Maddock}$) and the flow rate through bin *i* (Q_i).

$$p_{Q_i} = \frac{Q_i}{Q_{Maddock}} \qquad 11$$

S_Q is calculated with:

$$S_Q = \frac{-\sum_{i=1}^{M} p_{Q_i} \ln p_{Q_i}}{\ln M} \qquad 12$$

It is recommended to choose a bin distribution with a flow rate distribution significantly better than the mixing quality ($S_Q >> S_{rel}$), and preferably a bin distribution with equal flow rate through each bin ($S_Q \approx 1$). A method to check the flow rate in each bin is discussed in section 3.7.

Conclusion: bin size distribution

In conclusion, a bin distribution scheme with varying flow rates in the bins may result in a falsely high or low Shannon entropy (for the mix quality). Therefore, it is recommended to choose a bin distribution scheme with a homogeneous flow rate distribution. Whether the flow rate distribution is homogeneous in the bins can be checked with the Shannon entropy for flow rate (S_Q).

3.5 Uncertainty in Shannon entropy calculations due to a finite number of particles

The importance of particle count in Shannon entropy calculations is the primary focus of this section. A higher particle number increases the precision of the results, reducing both systematic and random errors. This section aims to explore and quantify these error contributions, to provide a model for calculating uncertainty and recommend criteria to keep both the systematic error and random error below 0.01.

First an example of Shannon entropy calculations with varying amounts of particles is shown with both a systematic and random error.

Subsequently, this model is expanded with varying number of bins and particle distributions to investigate the systematic and random errors due to a low number of particles.

Following this investigation, a model for uncertainty estimation in Shannon entropy is introduced.

The section concludes with targeted recommendations, ensuring a low systematic error and random error (<0.01).

Probability, resolution, and impact on Shannon entropy

Each particle in a bin represents a 1/*N* probability, this probability increases with decrease of *N* (*N* = number of particles). Therefore, an increase in *N* also increases the resolution with which the probability is determined. This results in more scatter in the Shannon entropy with a lower *N*. The impact on the Shannon entropy also depends on the total number of particles in a bin due to the log(p_i) part of the equation. The $p_i \cdot \log(p_i)$ changes more with the same change in probability if the probability is low. For example, $p_a \cdot \log(p_a)$ reduces with 0.014 when the number of particles in bin *a* reduces from 2 to 1 with *N* = 100, while $p_b \cdot \log(p_b)$ reduces with 0.006 when the number of particles in bin *b* is reduced from 10 to 9. The difference in resolution is 2.4 times higher between bin *a* and *b*. This may result in an error in the Shannon entropy with a low *N* even at an average of several samples (Shannon entropies). This is illustrated with an example in Figure 20.

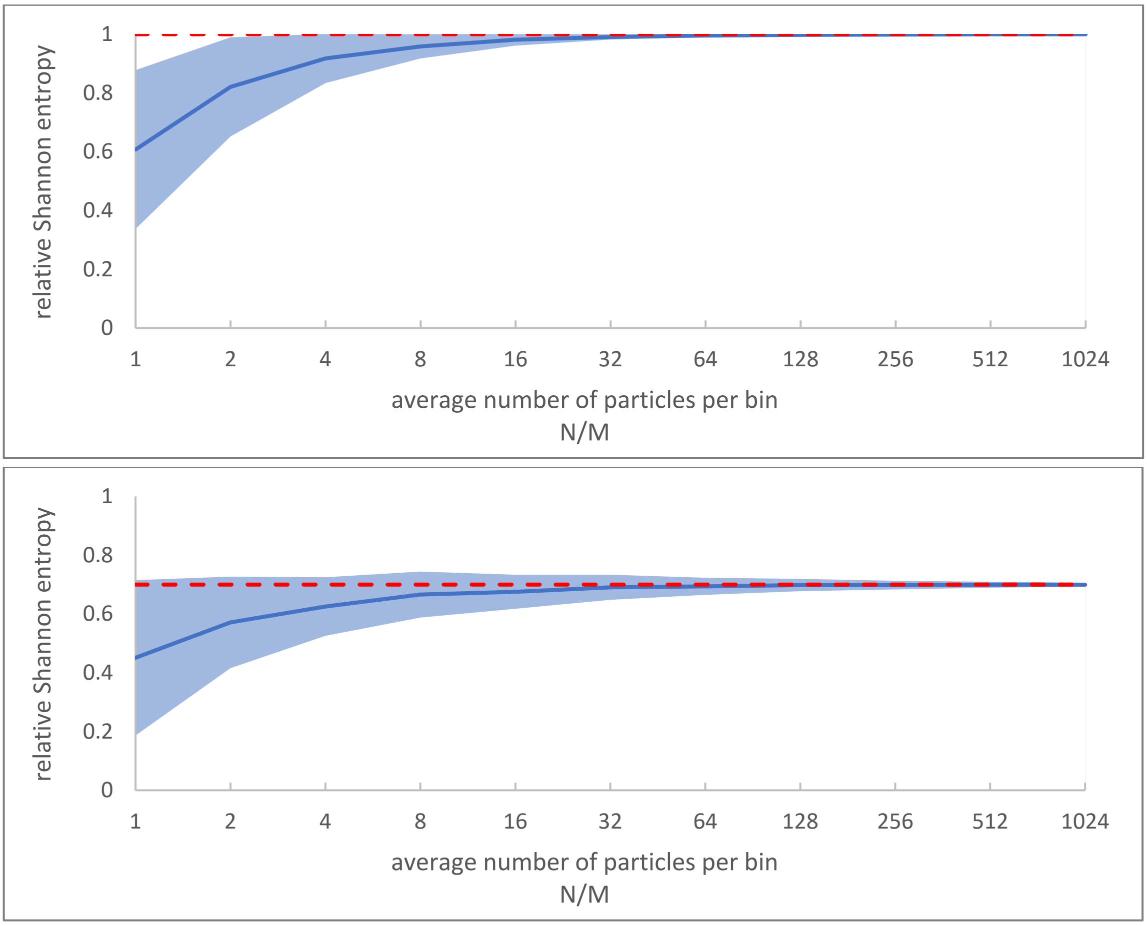

Figure 20. Average relative Shannon entropy, of 1000 samples, as a function of the average number of particles per bin with 3 bins. Upper figure: $S_{rel}(N = \infty) = 1$. Lower figure: $S_{rel}(N = \infty) = 0.7$. The red dotted lines show the relative Shannon entropy with $N = \infty$ ($S_{rel}(N = \infty)$), the blue lines show the Shannon entropy averaged over 1000 samples, the blue band shows the standard deviation over the 1000 samples.

Model-Based approach for Shannon entropy calculation

The Shannon entropy calculations in this example were done with a model system of 3 bins. Individual particle behavior was determined using a random number generator, no mixing simulations were needed. This system is a model, it does not represent a physical system like an extruder. These calculations however do show the behavior of Shannon entropy calculations at different particle numbers. The conclusions based on these calculations are applicable to all Shannon entropy calculations, including calculations with mixing simulations.

Systematic and random errors in Shannon entropy calculation

The Shannon entropy was calculated 1000 times, Figure 20 shows the average relative Shannon entropy and the standard deviation (σ). The example shows two different models with 3 bins. The Shannon entropy was calculated with a finite number of particles ($S_{rel}(N < \infty)$), with a minimum of 3 particles up to 3072 particles. In the first model the particles were randomly distributed over the 3 bins ($S_{rel}(N = \infty) = 1$). In the second model the particles had a higher probability to end up in a single bin (bin x), and an equivalent low probability to end up in one of the other two bins ($S_{rel}(N = \infty) = 0.7$).

The Shannon entropy calculated with a finite number of particles ($S_{rel}(N < \infty)$ shows a systematic error (ε_s) and a random error (ε_r) to the Shannon entropy with infinite particles $S_{rel}(N = \infty)$:

$$S_{rel}\left(N = \infty\right) = S_{rel}\left(N < \infty\right) + \varepsilon_s + \varepsilon_r \qquad 13$$

Addressing uncertainties and errors in Shannon entropy calculation

The systematic error is the difference between the average Shannon entropy and Shannon entropy with infinite particles $S_{rel}(N = \infty)$, see Figure 20. When N, is low, the systematic error reduces with increasing N. The error of the first model ($S_{rel}(N = \infty) = 1$) is 0.4 with $N/M = 1$, the error of the second model ($S_{rel}(N = \infty) = 0.7$) is slightly lower at 0.24.

The random error, inherently stochastic, tends towards an average value of zero with a large number of observations. This concept is further elaborated in the Guide to the Expression of Uncertainty in Measurement (GUM) (see section 3.2.2) [37]. However, the uncertainty associated with this random error, which is represented by the standard deviation (σ), is not zero. This uncertainty is visualized as a light blue band in Figure 20. Whenever a standard deviation is mentioned in this report, it refers to the uncertainty in the random error. The standard deviation reduces with increasing N and is 0.27 for both models at $N/M = 1$.

Shannon entropy calculation have to be corrected for a significant systematic error [38]. An error of more than ~0.01 seems significant. Furthermore, uncertainty contributions due to a systematic error ($u(\varepsilon_s)$) and a random error ($u(\varepsilon_r) = \sigma$) should be included in the uncertainty budget of the Shannon entropy.

Investigation of uncertainty with different Models

The above example shows that the uncertainty of a Shannon entropy calculation reduces with increasing number of particles. It also shows that the uncertainty differs with different Shannon entropies ($S_{rel}(N = \infty)$). The calculations were conducted iteratively using various models to estimate the ε_s and ε_r at different Shannon entropies ($S_{rel}(N = \infty)$).

These models featured distinct configurations, each characterized by a specific set of parameters:

- Number of bins (M): 3, 6, 12, 24, 48, 96, 192, 384, 768
- Average number of particles per bin (N/M): 2, 4, 8, 16, 35, 64, 128, 256, 512, 1024
- $S_{rel}(N = \infty)$ = 0.1, 0.2, 0.3, 0.4, 0.5, 0.6, 0.7, 0.8, 0.9, 1

990 different models in total, 1000 calculations per model in order to determine an average Shannon entropy and a standard deviation. The probability of a particle to end up in a specific bin i, was determined numerically with GNU Octave. The goal is to estimate the $\varepsilon_s \pm u(\varepsilon_s)$ and $\varepsilon_r \pm u(\varepsilon_r)$ as a function of N, M and S_{rel}. Therefore, the standard deviation for all 990 models are shown as a function of number of particles (N) in Figure 21. The error (ε_s) as a function of the average number of particles per bin (N/M) is also shown in Figure 21.

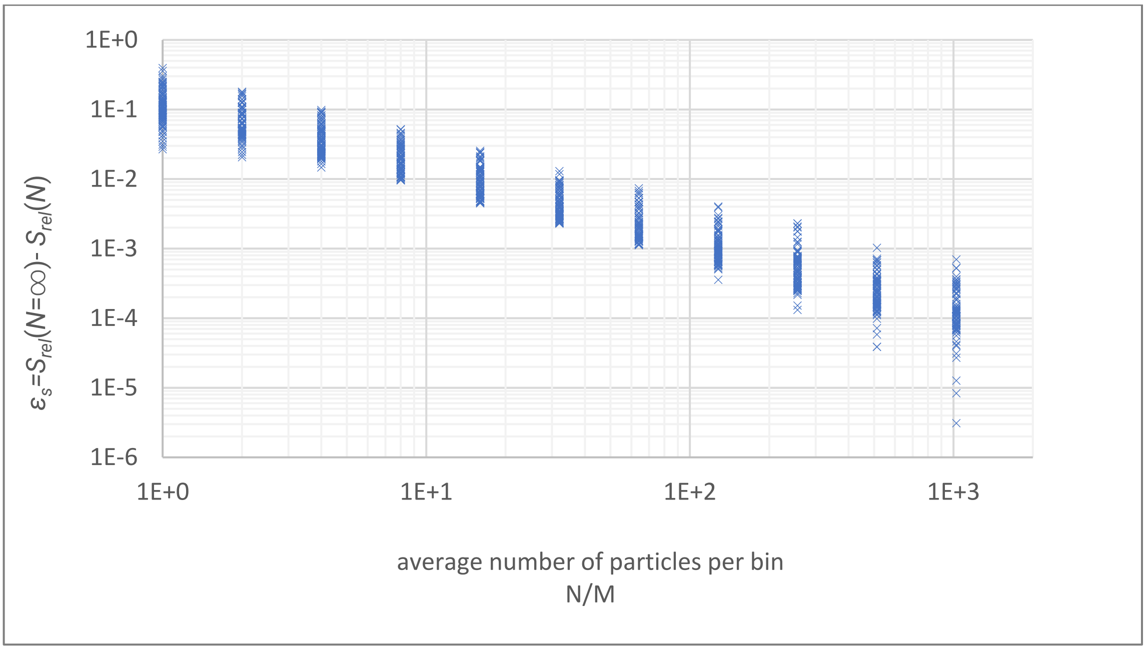

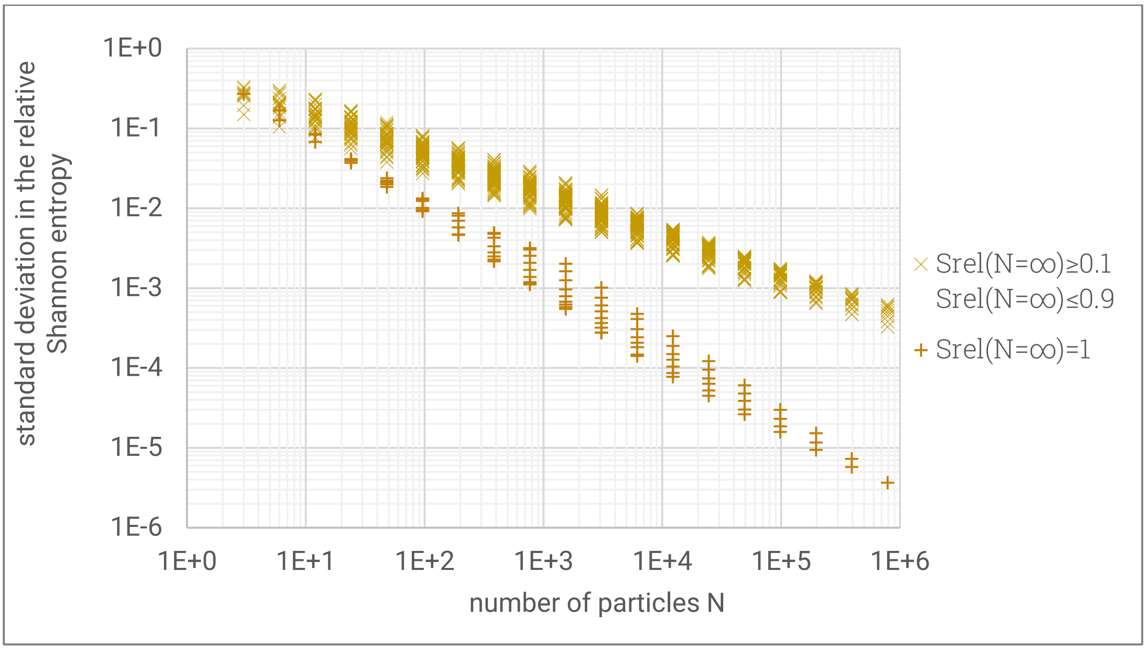

Figure 21. Upper figure: systematic error in $S_{rel}(N)$ as a function of N/M. Lower figure: standard deviation in the average $S_{rel}(N)$ as a function of the number of particles (N). Note: both horizontal and vertical axis are on a logarithmic scale.

Proposed criteria for Shannon entropy calculations

The systematic error in $S_{rel}(N)$ is inversely proportional to the average number of particles per bin (N/M). The standard deviation is a power function of the number of particles (N). At $N/M \geq 32$ the error in $S_{rel}(N)$ reduces to an insignificant amount of $\varepsilon_s \lesssim 0.01$ for all setups. Therefore, it is recommended to use $N/M \geq 32$ as a criterion for Shannon entropy calculations. Furthermore, it is recommended not to correct the Shannon entropy for the systematic error, but to include the maximum systematic error (for $N/M \geq 32$) to the uncertainty budget ($u(\varepsilon_s) = 0.01$).

The standard deviation reduces to $\sigma \lesssim 0.01$ with $N \geq 3072$ for all setups. Therefore, it is recommended to use $N \geq 3072$ as a criterion for Shannon entropy calculations.

The combined standard uncertainty (u_c) in the Shannon entropy is expressed with equation 14.

$$u_c^2 = \left(\frac{\partial S_{rel}(N=\infty)}{\partial \varepsilon_s}\right)^2 u^2(\varepsilon_s) + \left(\frac{\partial S_{rel}(N=\infty)}{\partial \varepsilon_r}\right)^2 u^2(\varepsilon_r) \qquad 14$$

$u(\varepsilon_s)$ is the uncertainty in the systematic error. $u(\varepsilon_r)$ is the uncertainty in the random error, this is equal to the standard deviation ($u(\varepsilon_r) = \sigma$). The sensitivity coefficients (partial derivatives in equation 14) are 1 for both systematic and random error. Therefore, the combined standard uncertainty can be calculated with equation 15.

$$u_c = \sqrt{u^2(\varepsilon_s) + u^2(\varepsilon_r)} \qquad 15$$

Conclusions and recommendations for the number of particles and uncertainty in Shannon entropy calculations

Summarizing, the number of particles affects the accuracy of Shannon entropy calculations. Both systematic error and random error increase with decrease in the number of particles (N) and the number of particles per bin (N/M). It is recommended to use $N/M \geq 32$ and $N \geq 3072$ as criteria for Shannon entropy calculations to ensure the systematic error and standard deviation fall below the significant threshold of 0.01. Furthermore, it is recommended to ad $u(\varepsilon_s) = 0.01$ to the uncertainty budget for the systematic error.

3.6 Shannon entropy for comparison between different extruders

Shannon entropy is a measure of distributive mixing. The Shannon entropy can be used to compare the distributive mixing quality between different extruders. Comparison between a wide range of extruders might be possible, but the focus of this study is on a comparison of different screw geometries, but with the identical screw diameter and length of the mixing . A method for processing the Shannon entropy and how to compare the different extruder is explained in this paragraph.

3.6.1 Tracer particle inflow section size

Paragraph 3.2 discusses a method of calculating the Shannon entropy for particles that flow in the extruder from a small section of the fluid inflow. The Shannon entropy can be calculated several times, each with a different particle inflow section. Figure 22 shows an example of a single extruder with the Shannon entropy calculated four times, each with another section for introducing the particles.

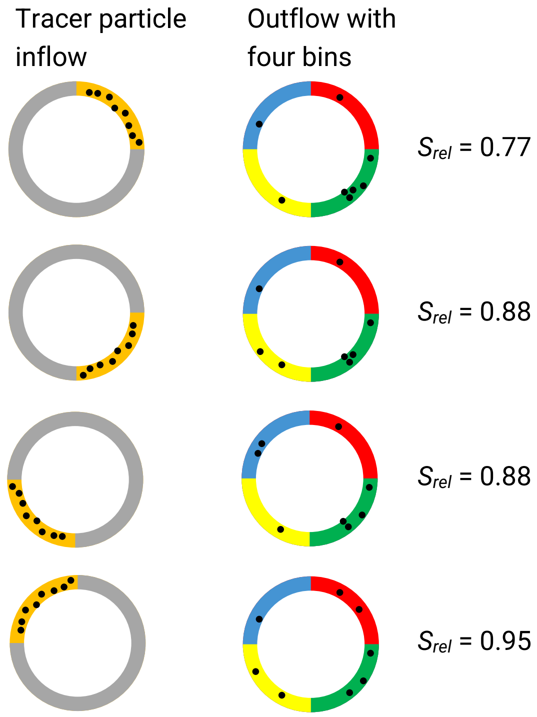

Figure 22. An example of a single extruder with Shannon entropy calculated four times, each with another section for introducing the particles.

Calculating the Shannon entropy for each inflow section is especially relevant when the mixing behavior is not homogeneous. How to process multiple Shannon entropies is discussed in paragraph 3.6.2.

It is recommended to have similar properties of the particle inflow sections for processing the Shannon entropies. This includes the flow rate, the area and the shape of the inflow sections. Overlap between inflow sections is not efficient, since overlap will result in including the same information multiple times. Therefore, a division without overlap is recommended. Paragraph 3.3 shows that a particle inflow section should not be larger than a single outflow bin. Therefore, the number of particles inflow sections should be at least as high as the number of bins if Shannon entropies are calculated for the whole inflow. The inflow sections in the example of Figure 22, meet all these requirements including size, shape, no overlap between inflow sections and number of sections. The example shows 4 bins and 4 particle inflow sections. Each particle inflow section contains 8 particles, that is 32 particles for all the inflow sections put together.

Introducing particles in a small section is time consuming with mixing simulations. It is more time efficient to introduce a large number of particles across the whole inflow (all inflow sections at once). Whether a particle originates in an inflow section is determined afterwards. For the Shannon entropy calculation of a specific inflow section only the particles from that specific inflow section are included. With this method the tracer particles in the simulation only have to be introduced once for all Shannon entropy calculations. Looking at the example (Figure 22), 32 tracer particles were introduced. The inflow is divided into 4 sections, each containing ¼ of the particles, that is 8 particles per section. But the same particles could also be used again for a different bin division scheme and Shannon entropy calculations. For example, a 3 bin division scheme, with 3 inflow sections and ~11 particles per inflow section.

The number of particle inflow sections reduces with increasing section size. A low number of particle inflow sections results in more particles per inflow section and therefore a higher number of particles per Shannon entropy calculation. The accuracy of each Shannon entropy calculation increases with an increase in the number of particles. Therefore, it is recommended to use large particle inflow sections. Paragraph 3.3 shows that a particle inflow section should not exceed that of one single outflow bin. Thus, the maximum advisable size for an inflow section is equivalent to one outflow bin.

3.6.2 Averaging Shannon entropy calculated with particles from multiple inflow sections

Shannon entropy can be used to compare distributive mixing between different extruders. The difference between extruders might be in the extruder setting (temperature, flow rate), or the geometry of the mixer. It seems evident that all other parameters should be the same between the extruders for making a reliable comparison. Therefore, it is recommended to have similar properties of the Shannon entropy calculation when comparing between extruders, this includes:

- Number of bins
- The size of the bins
- The size of the tracer particle inflow section
- The number of tracer particle inflow sections
- The number of tracer particles

Paragraph 3.6.1 shows how to divide the inflow into several sections. Tracer particles are introduced in each section for Shannon entropy calculations. These Shannon entropies may differ from each other. In the example, Figure 22, the inflow is divided into 4 sections, 4 Shannon entropies are calculated: 0.77, 0.88, 0.88, 0.95. With this method there are always several Shannon entropies per extruder. Several Shannon entropies per extruder makes comparison with other extruders difficult. For example, comparing two hypothetical extruders with the same number of bins, tracer particles and particle inflow sections. The example in Figure 22 is the first extruder, the Shannon entropies of both extruders are shown in Table 1. Note these this is a hypothetical example to illustrate handling of multiple Shannon entropies, the extruders do not have specific properties related to the hypothetical Shannon entropies.

Table 1. Shannon entropies of 2 extruders.

	Extruder 1 (Figure 22)	Extruder 2
Tracer particle inflow section 1	0.77	0.72
Tracer particle inflow section 2	0.88	0.93
Tracer particle inflow section 3	0.88	0.95
Tracer particle inflow section 4	0.95	0.93

The 4 Shannon entropies of each extruder do not compare easily. It is preferred to have a single value for each extruder and compare those to each other. If a minimum mixing quality is required, the minimum Shannon entropy of each extruder seems the best value for comparison between the two extruders. Minimum Shannon entropy of extruder one is 0.77, and 0.72 for extruder two. In this comparison extruder one is the better mixer.

Another comparison scheme is with the average of all Shannon entropies of an extruder. That is the average Shannon entropy of all the inflow sections of a single extruder. The average represents mixing behavior of the whole extruder, and might therefore be preferred to the minimum Shannon entropy comparison scheme. The inclusion of a standard deviation gives a measure of scatter that can be associated with each extruder. The average Shannon entropy of extruder 1 is 0.87 with a standard deviation of 0.06, the average Shannon entropy of extruder 2 is 0.88 with a standard deviation of 0.09. In this comparison extruder two is the better mixer. But the difference is very minor especially considering that the standard deviation is much larger than the difference between the two extruders.

Conclusion to Shannon entropy comparison methodology

In conclusion, the extrusion mixing quality may differ based on the chosen particle inflow section. For the evaluation of diverse mix qualities, two distinct analytical strategies are proposed. One approach centers around the utilization of minimum Shannon entropy, ensuring compliance with the baseline mixing quality requirements. Alternatively, the application of the average Shannon entropy offers a broader perspective on the overall performance characteristics of each extruder.

3.7 Particle tracking in Ansys CFX and Shannon entropy calculation with GNU Octave

This section provides an overview of the procedures involved in determining mix quality in extrusion simulations, focusing on the use of tracer particles and the analysis of their paths to calculate the Shannon entropy.

Tracer particle tracking in CFX simulations

Particle tracking of a CFX simulation can be done in CFD Post. The predetermined number of particles flow from a selected surface. In CFX Post the maximum number of tracer particles is 10^5. The particles have a one way interaction with the fluid. This means that the fluid determines the flow path of the tracer particles while the particles do not have any influence on the behavior of the fluid. The path of each particle is determined by calculating the next particle position with the velocity and trajectory of the fluid at the current particle position. This results in a series of positions of each particle. Calculating the tracer particle paths can take several hours. Ansys can create a text file with particle positions, time, fluid shear rate, velocity. These are large text files ($\sim 10^{10}$ byte).

Data processing: handling large datasets with GNU Octave scripts

To analyze such large amount of data GNU Octave scripts were developed for the extrusion simulations of this project. GNU Octave is a programming language, akin to MATLAB, commonly used in scientific computing. It allows for processing large datasets. With GNU Octave scripts the Shannon entropy, the number of particles for a Shannon entropy calculation and the average number of particles per bin (only the bins occupied with any particles are included in the average) was calculated.

Ensuring equal flow rate: verification and importance

The flow rate through each bin should be equal, see section 3.4.2. This requirement is verified by calculating the average axial velocity in each bin. The axial velocity in each bin is determined with a GNU Octave script, it averages the axial velocity of each tracer particles in each bin. The flow rate through each bin can be checked by dividing the axial velocity by the area of a bin.

An equal flow rate into each inflow section is also preferred, see section 3.6. This can be checked by meeting the required $S_Q \approx 1$. S_Q is calculated with the above mentioned GNU Octave script.

Conclusion: from tracer particles production to Shannon entropy calculation

In conclusion, tracer particles are produced with Ansys CFD post. This results in large datafiles (~10^{10} byte). GNU Octave script uses these files to calculate the Shannon entropy.

3.8 Conclusions and recommendations for Shannon entropy calculations

Distributive mixing in an extruder can be quantified with the Shannon entropy. The relative Shannon entropy is applicable when comparing distributive mixing of multiple extruders. A high Shannon entropy represents high distributive mixing quality, low mixing quality is represented by a low Shannon entropy.

Quantifying distributive mixing with Shannon entropy

The outflow surface of an extruder needs to be divided into several bins (M) in order to determine the Shannon entropy. The Shannon entropy is calculated with the number of tracer particles (N) that flowed through each bin. The tracer particles have to be introduced in a section of the inflow, this section is the same size as a single bin in the outflow surface. A tracer particle inflow section of a larger size than a single outflow bin will result in increase in the Shannon entropy which falsely suggest a higher mixing quality.

Importance of bin and inflow section size

The mixing effectiveness of the whole extruder mix section can be analyzed by using multiple particle inflow sections and calculating the Shannon entropy for each inflow section. The worst mixing of an extruder is represented by the minimum Shannon entropy of all the particle inflow sections. The minimum Shannon entropy can be used to compare different extruders. This is a comparison of the minimum mixing quality of each extruder. Another comparison scheme can be with the average Shannon entropy of all the particle inflow sections. With this comparison the overall better mixer can be found. Shannon entropy scatter should be considered when comparing the extruders, especially when the difference in average Shannon entropy is small.

Extruder comparison using minimum and average Shannon entropy

A higher number of tracer particles results in a reduction of the uncertainty in the Shannon entropy. The Shannon entropy shows a random error and a systematic error at a low number of particles (N). The random error reduces to $\lesssim 0.01$ with $N \geq 3072$ and the systematic error reduces to $\lesssim 0.01$ with $N/M \geq 32$. It is recommended to limit the Shannon entropy calculation to $N \geq 3072$ and $N/M \geq 32$.

Practical implications of tracer particle tracking in Ansys and GNU Octave

Tracer particles can be generated in Ansys CFD-Post, up to a maximum number of particles (*N*) of 10^5. As particle tracking in Ansys is time consuming, it is more efficient to introduce particles into all the inflow section simultaneously, rather than tracking them separately for each inflow section. The inflow section scheme can be applied via a GNU Octave script after particle tracking phase is complete. However, this method does have a drawback, it results in a reduced number of tracer particles for each Shannon entropy calculation. Furthermore, GNU Octave scripts have been developed for calculating the Shannon entropy.

The influence of bin number on scale of observation

The scale of observation depends on the number of bins. Mixing quality at a macroscopic level can be determined with a small number of bins. Mixing quality on a microscopic level can be determined with a high number of bins. It might be difficult to determine mixing quality at a high number of bins due to the limited number of particles (10^5) and the required minimum $N \geq 3072$ and $N/M \geq 32$.

The flexibility and implications of different bin distribution schemes

Several bin distribution schemes are possible, for example an angular, radial or a 2 dimensional bin distribution scheme. Information about distributive mixing in specific direction(s) can be determined with a specific bin distribution. The bin distribution should be chosen for specific mixture requirements. Possible several bin distribution schemes can be used to determine mixing quality in several directions.

4 General methods for residence time distribution to quantify axial mix quality

This section presents the RTD (residence time distribution) as a tool for quantify distributive mixing in single screw extruder simulations. How the RTD was applied in other studies is briefly shown in paragraph 2.1. In contrast to the previous section which addressed radial and angular mixing, this section will focus on the axial direction, i.e., along the length of the extrudate.

A unit of fluid, or an additive unit resides for some time in the extruder. Distributive mixing in the axial direction results in a difference in residence time (RT) among units of fluid/additive units. The difference in residence time increases with increase in axial distributive mixing. This can be shown with the residence time distribution (RTD).

Quantifying the RTD for a comparison between mixers

The RTD has to be quantified for a quantitative comparison between mixers. Two methods to quantify the RTD are considered the standard deviation of the residence time, and the Shannon entropy. Both are a single value measure of axial mix quality. The Shannon entropy used in this context is a measure of RTD, not of angular or radial distribution, hence is referred to as RTD Shannon entropy to differentiate from angular or radial Shannon entropy discussed in the previous section.

Both Shannon entropy and standard deviation is relatively easy to implement with GNU Octave scripts.

Shannon entropy calculation of the RTD

For the Shannon entropy bins are needed similar to a histogram of the residence time. With p_i the change of particle to end up in bin *i*. A bin is a range of particle residence time, for example all particle with 0 s < RT < 1 s end up in bin(0-1). The Shannon entropy is calculated with equation 1.

It might be that the highest particle residence time is significantly higher than the previous residence time. Many bins might not contain any particles if the range of bins include the highest particle residence time. Therefore, it seems reasonable to have a limited range of bins and not include any particles with a very high residence time. The uncertainty in RTD Shannon entropy calculations increase with a low number of particles, see also paragraph 3.5. The number of particles for Shannon entropy calculation is preferably $N > 3072$ and the number of particle particles per bin $N/M > 32$.

Average RTD and simulation

The average RTD is not a measure of mixing quality, but can be used as a check for simulation quality. The average RTD is the flow rate divided by the volume of the spiral Maddock.

$$\text{average residence time} = \frac{\text{volume}}{\text{flow rate}} \qquad 16$$

Conclusion RTD as a measure of axial mix quality

In conclusion, axial distributive mix quality can be determined with RTD. 2 methods are available for quantifying the mix quality: standard deviation in the RT and RTD Shannon entropy.

5 General methods to quantify dispersive mixing

This section is focused on a method to determine dispersive mix quality.

Shear stress as a measure of dispersive mix quality

With dispersive mixing an additive unit is broken up. The number of additive units increases while the individual additive unit size decreases. The additive unit can be a solid, such as carbon black agglomerates, or an immiscible fluid, such as an incompatible polymer. Shear stress beyond a critical value results in break-up of additive units, see also section 2 of part 1: ***Simulation Method*** [39]. A higher shear stress will result in a better dispersive mix quality. Therefore, dispersive mix quality was determined with the shear stress in the simulation.

Use of tracer particles in simulating dispersive mix quality

A tracer particle can be added to the simulation as a representation of an additive unit. The maximum shear stress experienced by such particle is the maximum shear stress that an additive unit would have experienced, and therefore represent the dispersive mix quality of this unit of fluid.

High shear stress at isolated points within the simulation does not offer a comprehensive understanding of the mix quality throughout the entire mixing section. When considering fluid flow through the extruder, some fluid segments may traverse regions characterized by high shear stress, resulting in enhanced dispersive mixing. In contrast, other fluid segments may primarily flow through areas with low shear stress, leading to suboptimal dispersive mixing. Therefore, analyzing the entire mixing section is essential for a precise evaluation of dispersive mix quality. One effective approach for this type of analysis involves the use of tracer particles, uniformly distributed across the inflow.

The tracer particles can be the same as used for distributive mix quality. Ansys CFD-Post generates those tracer particles and can also export the shear stress at each position of the tracer particles. The maximum shear stress of each particle can be determined by processing the data files with a GNU Octave script.

Comparing mixers using histogram of maximum shear stress

Several mixers can be visually compared in a histogram of the maximum shear stress of the tracer particles. The better dispersive mixer is the mixer where more particles experience a higher shear stress.

Conclusion: dispersive mixing

In conclusion, the section outlines a comprehensive method to evaluate dispersive mix quality, primarily using the measure of shear stress. The use of tracer particles offers a nuanced understanding of mixing quality, accounting for the different paths that fluid might take through the extruder. The approach allows for a comparative analysis of different mixers, aiding in the selection of a mixer that results in a higher proportion of particles experiencing high shear stress and thereby better dispersive mix quality.

6 Quantifying mix quality based on flow simulations

The preceding sections introduced methods aimed at quantifying distributive and dispersive mix quality, with the goal of enabling comparisons between different mixers. To assess the effectiveness of these methods, they were applied to a spiral Maddock (see Figure 23), a mixer specifically engineered for dispersive mixing in single screw extruders. These tests incorporated a total of four variations in geometry, screw rotational velocity, and polymer temperature.

Figure 23. Extruder screw with a spiral Maddock mixing section. Fluid flow is from right to left.

Paragraph 6.1 outlines the hypothesis for this mixer comparison. Paragraph 6.2 adapts the general methods for determining mix quality to suit the spiral Maddock simulations. A spiral Maddock was already simulated, see section 5 of part 1: *Simulation method* [39]. Paragraph 6.3 presents the specific variations used in the tests. Paragraph 6.4 provides a brief overview of all the methods applied to determine mix quality, concluding this section.

The subsequent section (7) presents the results of the mixer comparison, while the performance of the comparative methods is discussed in the conclusion (8).

6.1 Hypothesis

This paragraph discusses, the shear stress in the spiral Maddock, hypotheses on dispersive mixing and distributive mixing.

Shear stress in the spiral Maddock

With a spiral Maddock all the fluid has to travel through the gap between the barrier flight and the barrel, see Figure 24. The high shear stress in this region is the main source of high dispersive mixing in a spiral Maddock.

There is a pressure flow and a strong simple shear flow in this gap due to the velocity of the flight with respect to the barrel.

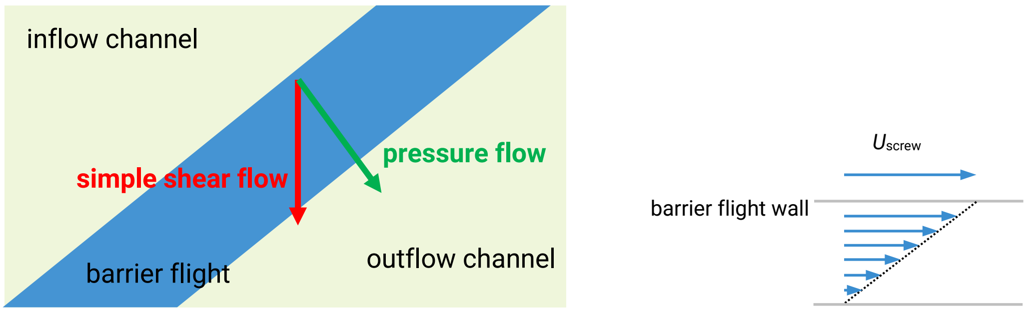

Figure 24. Schematic representation of simple shear velocity field in the gap between the barrier flight and the barrel.

The shear rate, due to the simple shear flow, in the gap is a function of the screw rotational velocity (ω), the barrel radius and the gap size. The shear can be calculated analytically without simulations:

$$\dot{\gamma} = \frac{R \cdot \omega}{gap} \quad (17)$$

Shear stress can be calculated with the power law and the above equation:

$$\tau = m\left(\frac{R \cdot \omega}{gap}\right)^n \quad (18)$$

Dispersive mixing

Equation 18 shows that the shear stress is both a function of gap size and screw rotational velocity. Therefore, an increase in the barrier flight height was expected to decrease dispersive mixing quality. Furthermore, an increase in rotational velocity was also expected to show an increase in dispersive mixing.

An increase in temperature results in a decrease in viscosity and shear stress. Therefore, an increase in temperature was expected to result in a decrease in dispersive mixing.

Distributive mixing

An increase in screw rotational velocity was expected to result in an increase in velocity gradient, and therefore an increase in distributive mixing in angular direction. Temperature was not expected to have a strong influence on distributive mixing.

6.2 Customized methods to determine mix quality

General methods for determining mix quality are shown in sections 3-5. The methods are not repeated here, but, for so far needed, customization for the spiral Maddock simulations is shown in this paragraph.

First the inflow position of the tracer particles is shown, then the specific bin distribution scheme for angular and radial Shannon entropy calculations. At last the specifics of the RTD calculations.

6.2.1 Tracer particle inflow

It is required that each particle represents the same amount of fluid for a proper representation of the fluid flow. This requirement is met with an equal distribution of particles at the inflow and an equal mass flow rate distribution at the inflow. The boundary conditions at the inflow results is an equal flow rate distribution. A large number of particles (10^5) were equally divided across the inflow.

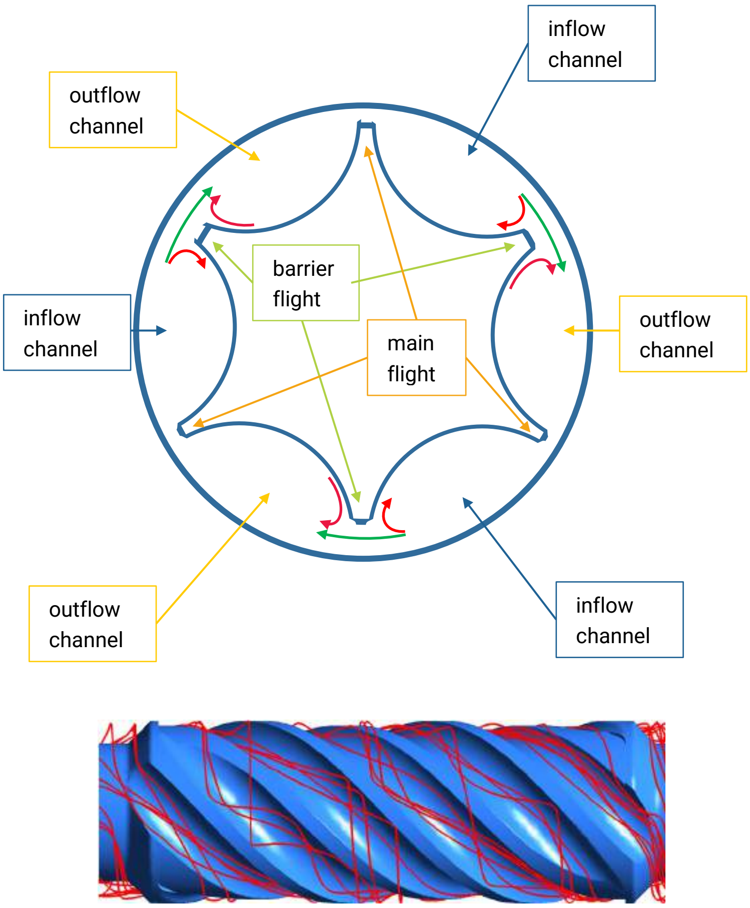

Figure 25. Upper: schematic cross section of a spiral Maddock. Lower: a small number of tracer particles in the spiral Maddock. Inflow is at the right, outflow at the left. The red lines show the flow paths of the tracer particles. The barrel and the fluid are not shown in this image.

The screw is discrete rotational symmetrical along the rotational axis. It consists of 3 equal sections. The barrel and boundary conditions are continues circle symmetrical along the same rotational axis. The screw mesh might not be symmetrical, but asymmetrical results were not observed in the mesh study, see section 5 of part 1: ***Simulation Method*** [39]. Therefore, equal behavior of the tracer particles is expected in each of the symmetrical parts. For more efficiency the particles are introduced into a one-third of the inflow.

6.2.2 Angular and radial Shannon entropy

Distributive mixing can be analyzed in several dimensions separately: angular direction, radial direction, and axial direction. Angular and radial distribution can be quantified with the relative Shannon entropy (S_{rel}), this is discussed in detail chapter 3. The terms 'radial Shannon entropy' and 'angular Shannon entropy' are used to emphasize the distinction between the radial and angular distributions.

Shannon entropy is determined at the outflow side of the spiral Maddock. Therefore, the outflow is divided into several bins.

A schematic of angular and radial bin division is shown in Figure 26.

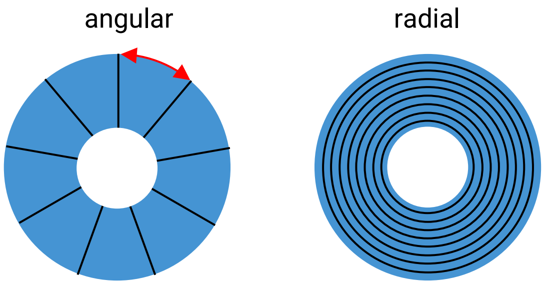

Figure 26. Schematic of bin distribution schemes. Left: angular divisions. Right: radial division.

The schematic shows a division with 8 bins. The typical size of the angular bins is the circumference divided by the number of bins, see the red arrow in the above figure. The typical size of the radial bins is the distance between the screw and the barrel divided by the number of bins. Mixing quality at a macroscopic level can be determined with a small number of bins. Mixing quality on a microscopic level can be determined with a high number of bins. Both large and small bin sizes were used, see Table 2.

Table 2. Number of bins and typical bin size

bin division scheme	number of bins (M)	typical size [mm]
angular	3	79
angular	6	39
angular	12	20
angular	24	10
angular	48	4.9
angular	96	2.5
angular	192	1.2
angular	384	0.61
angular	768	0.31
radial	2	5.0
radial	4	2.5
radial	8	1.3
radial	16	0.63

The tracer particles are introduced in a section at the inflow of the spiral Maddock. The inflow section is of the same size and shape as an outflow bin, therefore the division of the inflow sections is equal to the bin divisions, see Figure 26. It is preferred to determine mixing quality of the whole spiral Maddock. Therefore, multiple particle inflow sections were used. Multiple Shannon entropies were calculated since there are multiple particle inflow sections.

6.2.3 Residence time distribution

The RTD method is described in section 4, is not reiterated here; this section focuses only on the aspects customized for the spiral Maddock.

Standard deviation

The standard deviation in the residence time, of the tracer particles, was calculated. There might be a small number of particles that have a very high residence time. A small number of particles do not have a great effect on the mix quality, but they might increase the standard deviation significantly. To cancel this effect the standard deviation was also calculated with only the particles with a residence time of less than 100 s, and once with all particles with less than 25 s residence time.

Shannon entropy of the residence time distribution

The RTD Shannon entropy was calculated with bin size 1 s. With bins starting from the lowest particle residence time (to be determined) up to RT = 100 s. Consequently, the number of bins is at maximum 100. The number of particles for Shannon entropy calculation is preferably $N > 3072$ and the number of particle particles bin $N/M > 32$ for accurate Shannon entropy calculations. The first requirement is easily met since 10^5 particles were used for the calculations. The second requirement is met if $M \leq 3125$, since $M \leq 100$.

6.3 Spiral Maddock simulation variations

Four different simulation setups were created, identical to the simulation reported in section 5 of part 1: *Simulation method*, except for the temperature, screw rotational velocity and the barrier flight height [39]. The variations in the spiral Maddock simulations are shown in this paragraph, an overview of the variations is shown in Table 3.

Table 3. simulation setups

Simulation number	Simulation name	Temperature [°C]	Screw rotational velocity [rounds per minute]	Gap between the barrier flight and the barrel [mm]
1	standard	200	14	0.74
2	high screw velocity	200	44	0.74
3	high temperature	250	14	0.74
4	lwered barrier flight	200	14	1.74

To the simulation is referred, in this report, with the simulation number or name as is shown in the above table.

The standard simulation (setup 1) is the exact same simulation as the simulation, with a 58 M cells mesh, reported section 5 of part 1: ***Simulation Method*** [39].

The variations in settings (screw rotational velocity, temperature, and barrier flight height) were chosen to determine whether this setting influences the mixing quality. Each value is an increase of the standard value, but not an expert choice. For example, the 50 °C temperature increase (simulation 3) was chosen since the temperature difference seems large enough to have a discernable impact on the rheological behavior of the fluid.

6.4 Brief overview of all applied methods

In prior sections of this work, various methods have been introduced and explored to determine mix quality in single screw extruders. This paragraph provides a summary of all the applied methods:

- Evaluation of angular and radial distributive mix quality as functions of particle inflow section and bin size
- Assessment of flow rate distribution homogeneity in both angular and radial bin distribution schemes
- Analysis of the RTD, standard deviation in residence time, and RTD Shannon entropy
- Verification of the requirements of $N/M > 32$ and $N > 3072$ for all Shannon entropy calculations
- Comparison of average residence time with analytical average residence time
- Construction of a histogram representing the maximum shear stress of each particle as a measure of distributive mix quality, and its comparison to analytical calculations of the maximum shear stress.

7 Results

The spiral Maddock simulations all converged, and the mix quality was determined using tracer particles. This section presents the results, beginning with a visual inspection of the particle distribution, followed by an analysis of angular and radial Shannon entropy, RTD, and dispersive mix quality.

7.1 Particle distribution

In one-third of the inflow of the spiral Maddock, 10^5 tracer particles were introduced. Figure 27 depicts the particle positions at the inflow of the spiral Maddock.

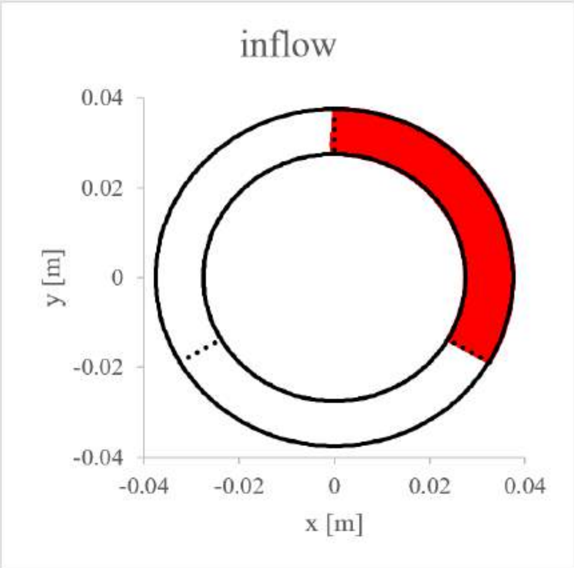

Figure 27. Tracer particles positions at the inflow. The particles are red dots, the number of particles (~10^5) is so high that individual particles cannot be distinguished from the bulk of the tracer particles. The tracer particle inflow section is marked with dotted lines.

The tracer particles, represented as red dots in Figure 27, are so numerous (~10^5) that individual particles cannot be distinguished from the bulk. The same holds true for the particle depiction in Figure 28. The inflow geometry and the tracer particle positions at the inflow are equal for the different simulation setups. 3 angular sections of the inflow are marked with dotted lines. The size and shape of an inflow section is equal to a single bin at the outflow. The inflow section in the above figure corresponds to angular Shannon entropy calculations with 3 angular bins. Figure 28 shows the tracer particle positions at the outflow for all the simulation setups.

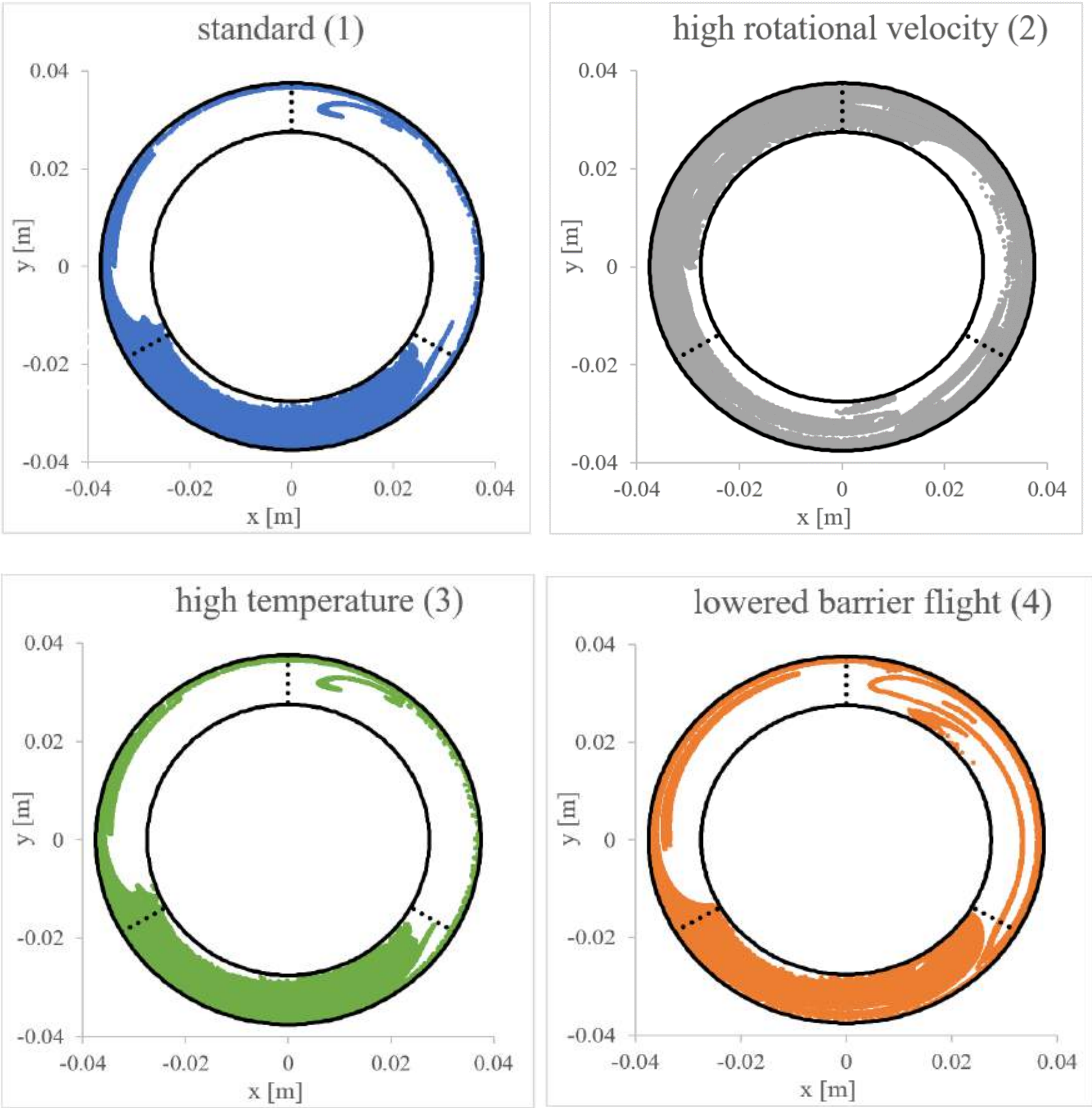

Figure 28. Tracer particles positions at the outflow of the spiral Maddock. The particles are colored dots, the number of particles (~10^5) is so high that individual particles cannot be distinguished from the bulk of the tracer particles. 3 angular bins are marked with dotted lines.

As in the previous figure, Figure 28 also features 3 angular bins marked with dotted lines. The figure gives an indication of mixing quality. Due to the inability to discern individual particle density in the given figures, it is important to note that variations in particle density distribution indicate changes in distributive mixing quality. All the simulations show an area without any particles (white area's). The high screw rotational velocity simulation (setup 2) shows the least white areas, this suggests a better distributive mixing quality compared to the other simulations. The standard simulation (setup 1) and the high temperature simulation (setup 3) show a very similar pattern, this suggests a very similar distributive mixing quality.

7.2 Angular Shannon entropy

The angular Shannon entropy was calculated with an angular bin. There are some requirements for the angular Shannon entropy calculations, whether the results meet these requirements is discussed in paragraphs 7.2.1 and 7.2.2. The results of the angular Shannon entropy calculations are discussed in paragraphs 7.2.3 to 7.2.5.

7.2.1 Angular flow rate distribution at the outflow

Difference in flow rate through each bin may result in an error in the angular Shannon entropy calculation. Therefore, the axial velocity at the outflow was examined. Figure 29 shows the axial velocity at the outflow of the lowered barrier flight simulation (setup 4), the other simulations show a similar flow pattern at the outflow.

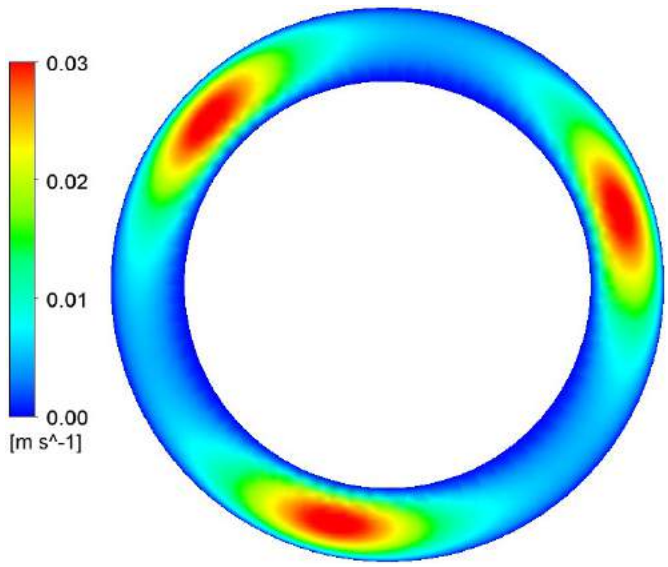

Figure 29. Axial velocity at the outflow of the simulation with the lowered barrier flight (setup 4)

The axial velocity distribution is not equal and therefore the flow rate distribution neither. The axial velocity is high near the outflow channels of the extruder. This axial velocity gradient in angular direction reduces with increased distance from the outflow channels. Therefore for future simulation studies it is recommended to increase the distance between the outflow of the simulation and the spiral Maddock outflow channels.

The flow rate distribution across the bins was quantified with the Shannon entropy for flow rate (S_Q). The same bins were used as for Shannon entropy calculations for distributive mixing. S_Q as a function of number of bins is shown in Figure 30.

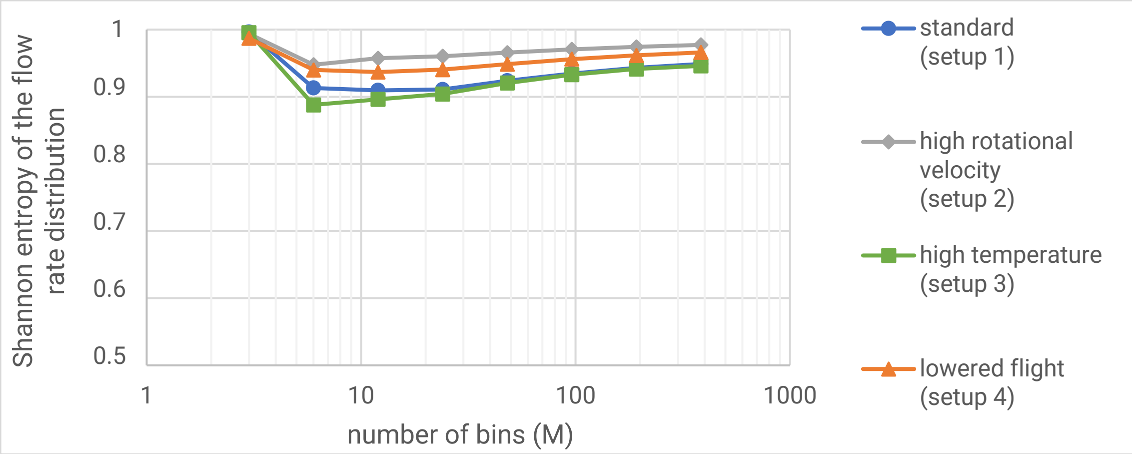

Figure 30. S_Q as a function of number of bins. The horizontal axis is on a logarithmic scale.

The required flow rate distribution is $S_Q \approx 1$ and $S_Q >> S_{rel}$. The first requirement is not met, though $S_Q \gtrsim 0.9$ is not far from $S_Q \approx 1$. The second requirement is further discussed in paragraph 7.2.4.

7.2.2 Number of particles for angular Shannon entropy calculations

The accuracy of angular Shannon entropy calculations is a function of the number of particles (*N*), and the average number of particles per bin (*N*/*M*). *N* and *N*/*M* were examined to estimate the accuracy of the angular Shannon entropy calculations. Figure 31 shows both *N* and *N*/*M* as a function of number of bins (*M*).

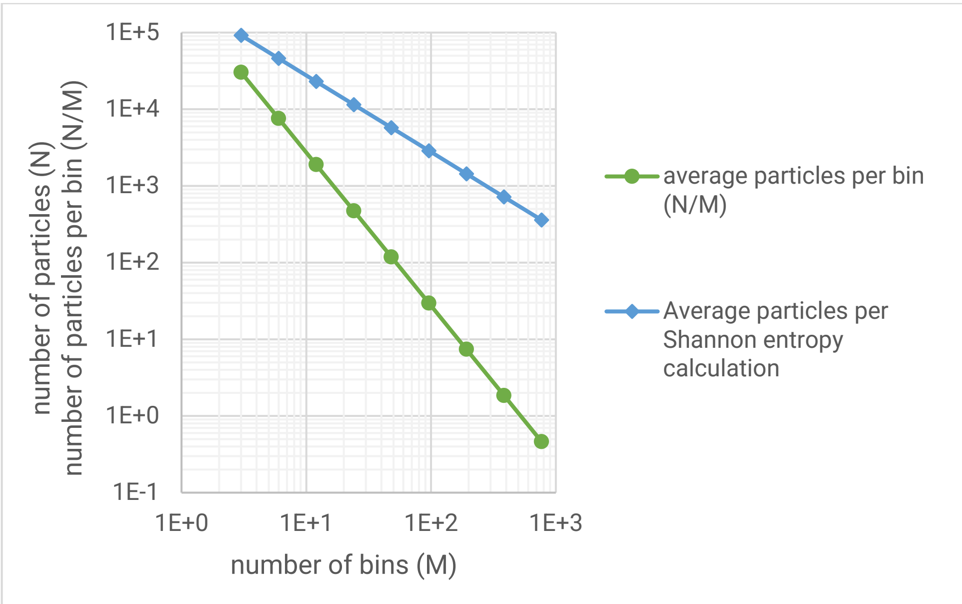

Figure 31. The number of particles for Angular Shannon entropy calculations (N) as a function of the number of bins (M). And the number of particles per bin (N/M) as a function of number of bins (M). Both N and N/M are and average of all the setups. Both axis is on a logarithmic scale.

The same amount of tracer particles and bins were used for all the setups. Therefore Figure 31 shows the average of all setups. $N/M > 32$ with $M \leq 96$, and $N > 3072$ with $M \leq 96$. Therefore, the systematic and random errors and their uncertainties are expected to be low for the angular Shannon entropy calculations at $M \leq 96$.

7.2.3 Angular Shannon entropy with 96 bins

The inflow of the spiral Maddock was divided into several sections. Tracer particles flow in at each section and angular Shannon entropy is calculated for each section. The division of the inflow is equal to the bin division at the outflow, a schematic of angular division is shown in Figure 26. Each inflow section has a begin and end angle, angular Shannon entropy as a function of inflow section angle is shown in Figure 32.

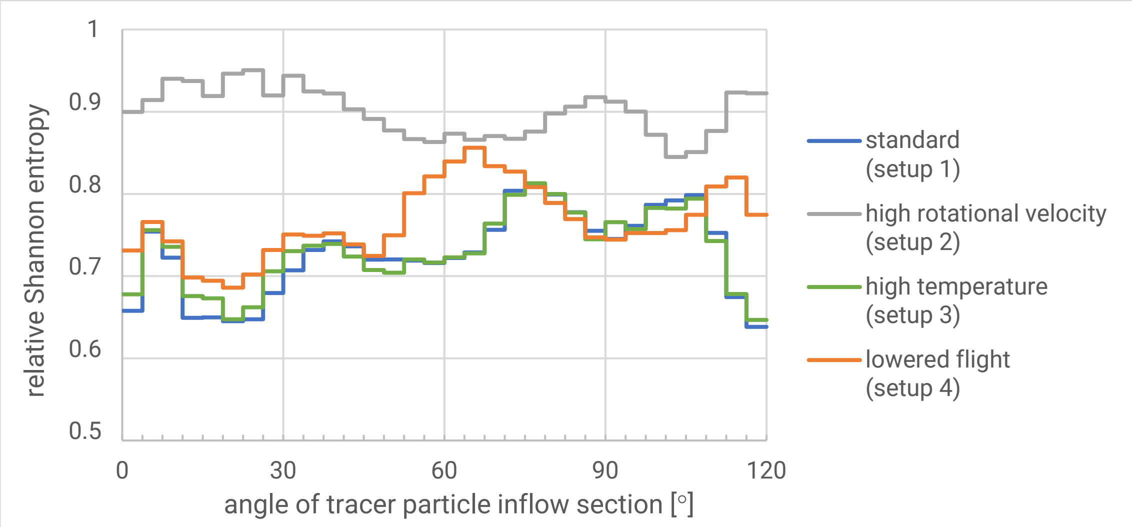

Figure 32. Shannon entropy as a function of inflow section angle with 96 bins.

The angular Shannon entropy is calculated multiple times with different numbers of bins, see Table 2. The above figure shows the results for 96 bins. The uncertainty in the angular Shannon entropy does not exceed 0.02 for 96 bins. The angular Shannon entropy and the distributive mixing quality depends on the tracer particle inflow section. For example the lowered flight simulation (setup 4): the mixing quality is better with inflow section at 60.75°-67.50° (S_{rel} = 0.86) while the mixing quality is less (S_{rel} = 0.73) with the inflow section at 0°-3.75°. This shows the relevance of calculating the angular Shannon entropy for each section of the inflow, and not only a single inflow section. Large differences in angular Shannon entropies result in a high standard deviation, and therefore a high uncertainty in the average angular Shannon entropy. The average angular Shannon entropy is discussed in paragraph 7.2.4.

7.2.4 Average angular Shannon entropy

Figure 33 displays the average angular Shannon entropy both as a function of number of bins and typical bin width.

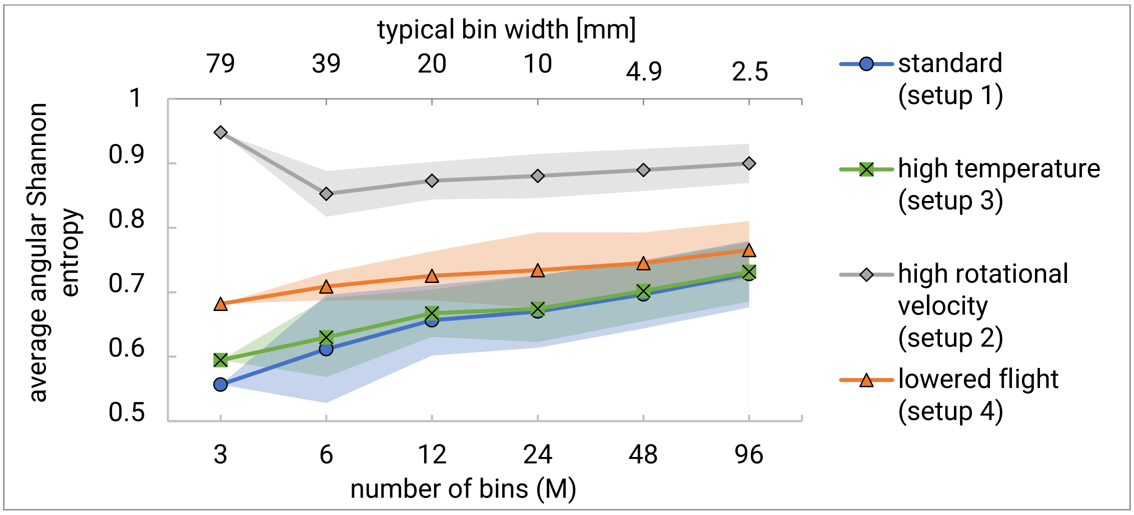

Figure 33. Average angular Shannon entropy as a function of number of bins. The continuous lines represent the average angular Shannon entropy, while the colored bands illustrate the uncertainty. The horizontal axis is on a logarithmic scale.

For setups 1, 3, and 4, the angular Shannon entropy is substantially lower than the flow rate distribution across the outflow bins (S_Q >> S_{rel}). The difference is less for setup 2. But the flow rate distribution is high for setup 2 ($S_Q \gtrsim 0.9$). Therefore, the flow rate distribution is not expected to have a significant influence on any of the angular Shannon entropy calculations.

The figure also shows the uncertainty in the average angular Shannon entropy. The uncertainty at M = 3 is underestimated, since there is only a single inflow section, therefore only a single angular Shannon entropy calculation and no standard deviation. The standard deviation is a large contribution to the uncertainty at other values of M.

As the number of bins increases, the angular Shannon entropy rises, yet for the majority of data points, this change does not hold significant weight considering the accompanying uncertainty.

The high rotational screw velocity simulation (setup 2) shows the highest angular Shannon entropy at all values of M. Therefore setup 2 is the best in angular mixing, this is in agreement with the expectations. The simulation with the standard setup (setup 1) and the simulation with the high temperature (setup 3) show almost the same angular Shannon entropy at all values of M. The simulation with the lowered barrier flight (setup 4) shows a bit higher angular Shannon entropy compared to the standard setup. But the results overlap when the uncertainty is considered, therefore it is not possible to conclude what setup is better.

In conclusion, the average angular Shannon entropy does provide information about what the better mixer is. Although this is limited due to the high uncertainty.

7.2.5 Minimum angular Shannon entropy

The minimum angular Shannon entropy as a function of number of bins is shown in Figure 34. The typical bin width is also shown in the figure.

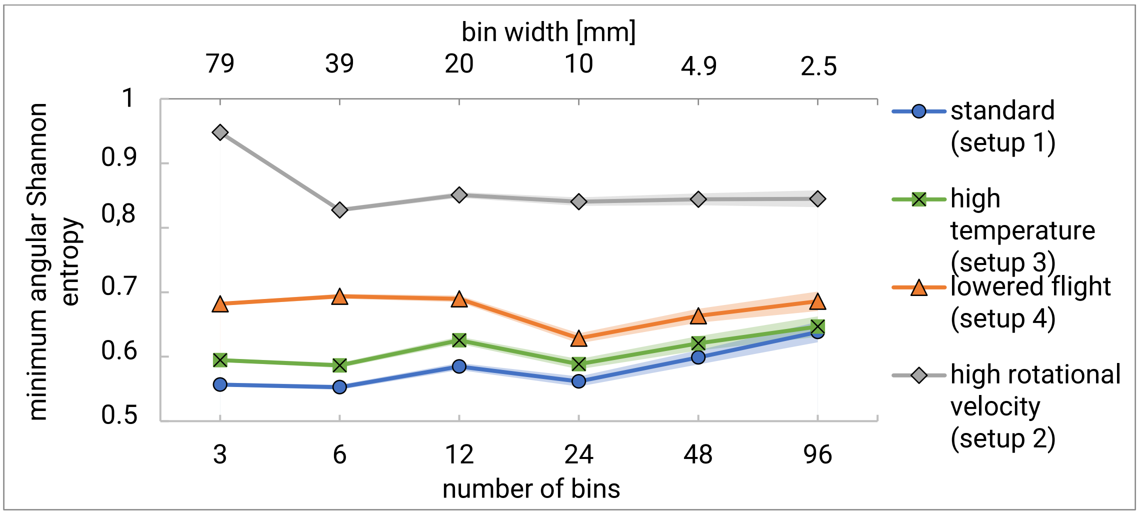

Figure 34. Minimum angular Shannon entropy as a function of number of bins. The continuous lines signify the minimum angular Shannon entropy, whereas the uncertainty is represented by the colored bands. The horizontal axis is on a logarithmic scale.

The uncertainty is lower compared to the average angular Shannon entropy (Figure 33), which is attributed to the high standard deviation associated with the average angular Shannon entropy.

The observations from setup 2, which displays the highest angular Shannon entropy at all values of *M*, align with expectations and suggest it provides the best angular mixing. A striking similarity is observed in the angular Shannon entropy values for both the standard setup (setup 1) and the high-temperature simulation (setup 3) across various *M* values. The simulation with the lowered barrier flight (setup 4) shows a bit higher angular Shannon entropy compared to the standard setup. But the results overlap at $M > 192$ if the uncertainty is considered.

In conclusion, the minimum angular Shannon entropy makes clear distinction between mixers and is therefore suitable method for comparing mixers.

7.3 Radial Shannon entropy

The radial Shannon entropy calculation employs a radial bin division as described in paragraph 6.2.2. There are certain criteria for the radial Shannon entropy calculations, and the extent to which the results meet these criteria is discussed in paragraphs 7.3.1 and 7.3.2. The results of the radial Shannon entropy calculations are discussed in paragraphs 7.3.3 and 7.3.4.

7.3.1 Radial flow rate distribution at the outflow

Difference in flow rate through each bin may result in an error in the radial Shannon entropy calculation. Axial velocity is discussed in paragraph 7.2.1. The radial flow rate distribution expressed with S_Q is discussed in this paragraph. The same bins were used for radial Shannon entropy calculations for distributive mixing. S_Q as a function of number of bins is shown in Figure 35.

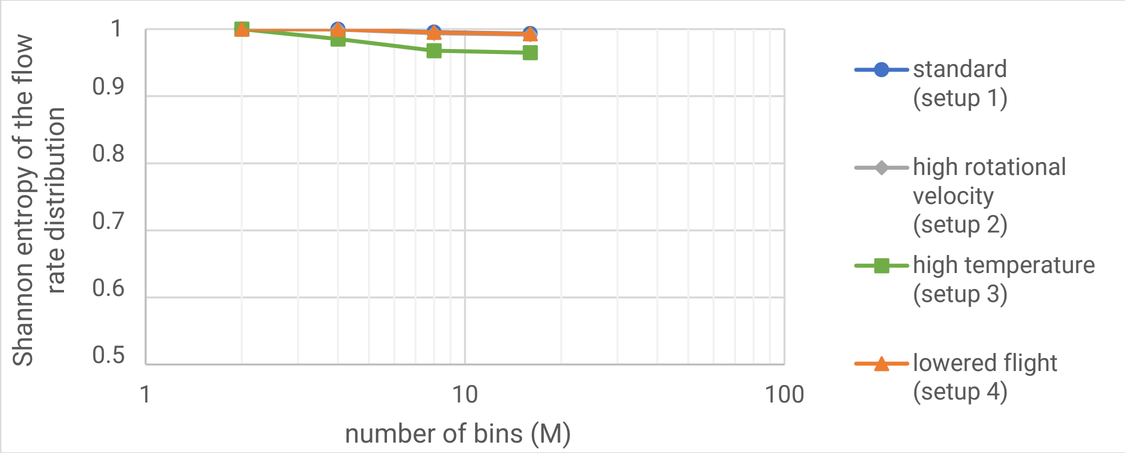

Figure 35. S_Q as a function of number of bins. The horizontal axis is on a logarithmic scale.

The required flow rate distribution is $S_Q \approx 1$ and $S_Q >> S_{rel}$. The first requirement is met with $S_Q \gtrsim 0.96$.

7.3.2 Number of particles for radial Shannon entropy calculations

The accuracy of radial Shannon entropy calculations is a function of the number of particles (*N*), and the average number of particles per bin (*N/M*). *N* and *N/M* were examined to estimate the accuracy of the radial Shannon entropy calculations. Figure 36 shows both *N* and *N/M* as a function of number of bins (*M*)

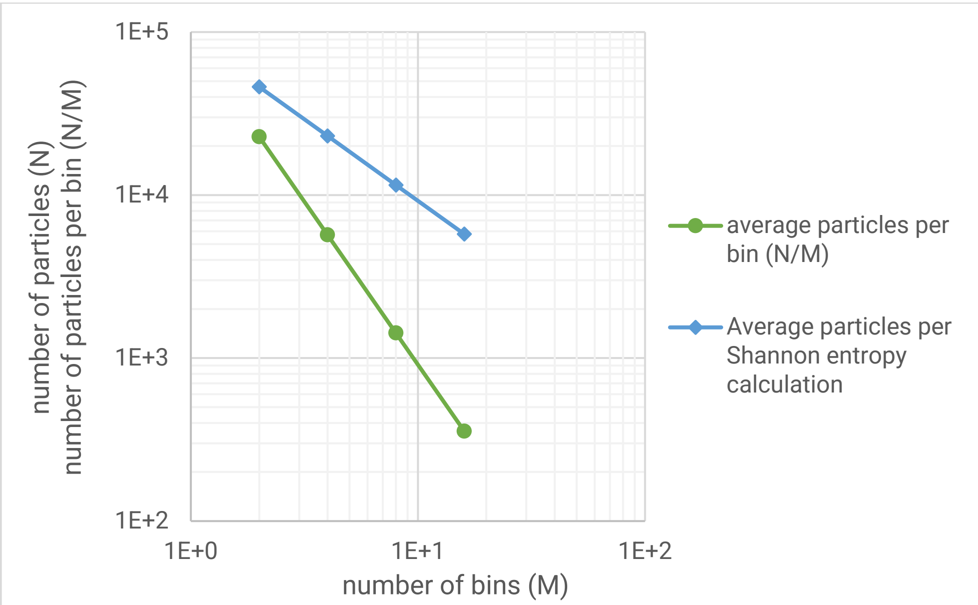

Figure 36. The number of particles for radial Shannon entropy calculations (N) as a function of the number of bins (M). And the number of particles per bin (N/M) as a function of number of bins (M). Both N and N/M represent an average of all setups. Each axis is on a logarithmic scale.

The same amount of tracer particles and bins were used for all the setups. Therefore Figure 36 shows the average of all setups. $N/M > 32$ and $N > 3072$ for all calculations. Therefore, the systematic and random errors and their uncertainties are expected to be low.

7.3.3 Radial Shannon entropy with 16 bins

The inflow of the spiral Maddock was divided into several sections. Tracer particles flow in at each section and radial Shannon entropy is calculated for each section. The inflow division mirrors the bin division at the outflow, as depicted by the angular division schematic in Figure 26. Each inflow section has a begin and end angle, radial Shannon entropy as a function of inflow section angle is shown in Figure 37.

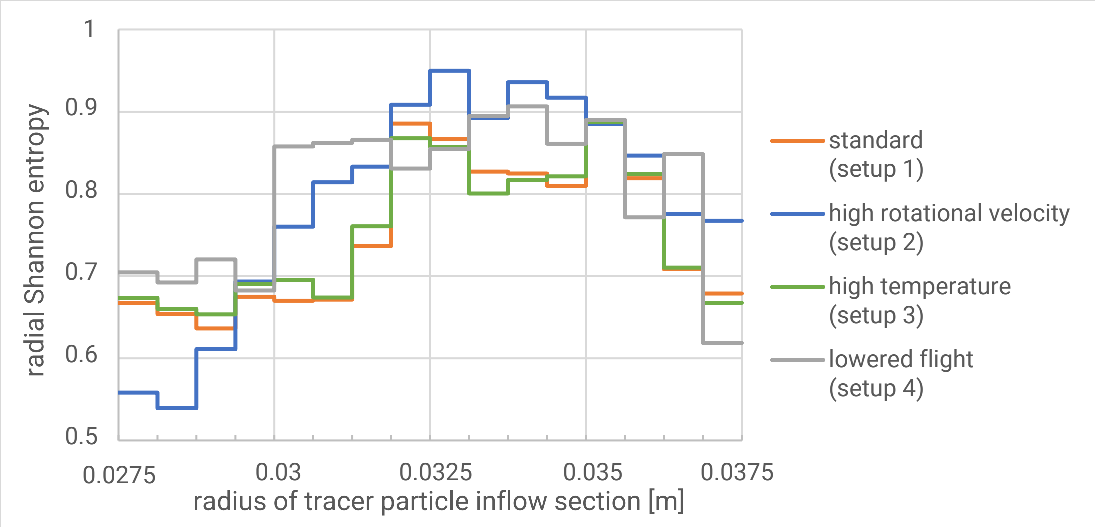

Figure 37. Radial Shannon entropy as a function of inflow section radius with 16 bins.

The radial Shannon entropy is calculated with different numbers of bins, see Table 2. The above figure shows the results for 16 bins. The uncertainty in the radial Shannon entropy does not exceed 0.02 for 16 bins. The radial Shannon entropy and the distributive mixing quality depends on the tracer particle inflow section. This shows the importance of calculating the radial Shannon entropy for each section of the inflow, and not only a single inflow section.

Large differences in radial Shannon entropies results in a high standard deviation, thus contributing to a significant uncertainty in the average radial Shannon entropy. The uncertainty in the average radial Shannon entropy is so high that no conclusions can be drawn from the average radial Shannon entropy. Therefore, the average radial Shannon entropy is not suitable for determining the most optimal radial mixer.

7.3.4 Minimum Shannon entropy

The minimum radial Shannon entropy as a function of number of bins is shown in Figure 38. The typical bin width is also shown in the figure.

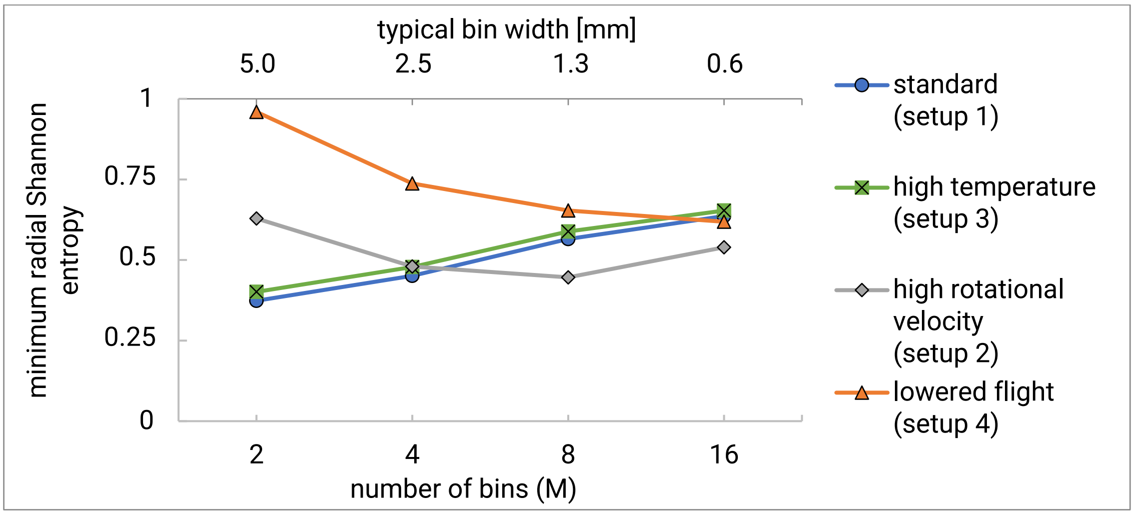

Figure 38. Minimum radial Shannon entropy as a function of number of bins. The horizontal axis is on a logarithmic scale.

The lowered barrier flight simulation (setup 4) shows the highest radial Shannon entropy at a low *M*. Therefore setup 4 is the best in radial mixing at a low *M*. All the simulations show almost the same radial Shannon entropy at $M = 16$.

The radial Shannon entropy of setups 2 and 4 reduce with increase of number of bins in contrast with the increase of radial Shannon entropy for setups 1 and 3. This was not further studied but might be an interesting subject for future work.

In conclusion the minimum radial Shannon entropy does show a clear difference between mixers and is therefore useful to find the most optimal radial mixer.

7.4 Residence time distribution

The residence time distribution (RTD) is a measure of distributive mixing in axial direction. The residence time of the tracer particles was determined and relevant statistical data are presented in Table 4.

Table 4. Tracer particle residence time per simulation setup.

Simulation setup	Average residence time [s]	Minimum residence time [s]	Maximum residence time [s]	Standard deviation [s]	Particles with a residence time of >100 s
standard (1)	12.7	7.9	345.4	4.1	2
high rotational velocity (2)	13.1	7.7	1548.5	8.1	20
high temperature (3)	12.7	7.9	133.2	3.9	2
lowered flight (4)	13.2	9.6	155.2	3.9	1

As the flow rate and volume are consistent across simulations 1 to 3, the nearly identical average residence times align with the equation 16. The lowered flight simulation (4) has a bit higher average residence time, which is also in agreement with equation 16 since the volume of simulation 4 is a bit higher.

The standard deviation serves as an indicator of RTD. Simulations 1, 3 and 4 have a standard deviation of ~4, while the high rotational velocity simulation (2) has a significantly higher standard deviation of 8.1. A higher standard deviation suggests a broader distribution and therefore better distributive mixing. The RTD is visualized with a histogram with a bin size of 1 s.

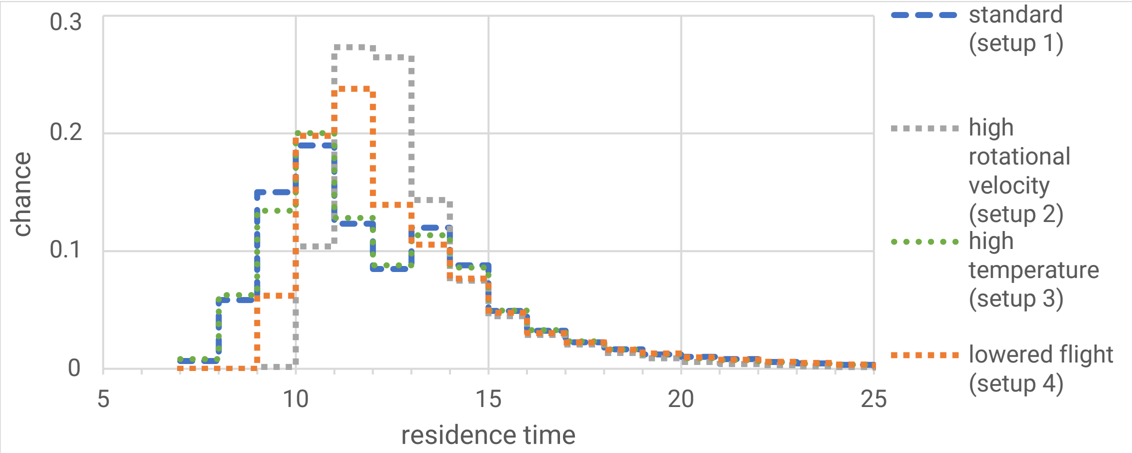

Figure 39. histogram of the tracer particle residence time in the spiral Maddock. The bin size is 1 s. Up to 25 s is shown in the histogram while the highest residence time is 1549 s.

The histogram shows a very similar distribution for all the setups. The high screw velocity simulation (2) shows a narrower distribution compared to the rest. This is in disagreement with the very high standard deviation of setup 2. The high standard deviation might be due to a small number of particles with a very high residence time. Setup 2 has much more particles with a very high residence time and the maximum residence time is much higher. This small amount of particles has an influence on the standard deviation, while the number of particles (20) seem too small for any significant influence on the distributive mixing behavior of all the particles (~10^5).

The standard deviation was recalculated for particles with a residence time of less than 25 s and excluding those with a residence time of more than 100 s. Only less than 2 % of particles have a higher residence time.

Table 5. Tracer particle residence time per simulation setup for particles with a residence time of less than 100 s.

Simulation setup	Standard deviation with residence time ≤ 25 s	Standard deviation with residence time ≤ 100 s	Shannon entropy of the RTD [-]
standard (1)	3.6 s	3.8 s	0.54
high rotational velocity (2)	3.6 s	3.7 s	0.44
high temperature (3)	3.6 s	3.8 s	0.54
lowered flight (4)	3.7 s	4.0 s	0.51

Once particles with high residence times are excluded, all simulations exhibit nearly identical standard deviations. Therefore, the standard deviation is not suitable for a comparison between mixer.

The RTD Shannon entropy was calculated as well. The bin size is 1 s for the RTD Shannon entropy calculations, the lowest bin is 7 s - 8 s, the highest bin is 99 s - 100 s, the total number of bins is 92. The number of particles for RTD Shannon entropy calculation is preferably $N > 3072$ and the number of particle particles bin $N/M > 32$. The first requirement is met with $N \approx 10^5$. The second requirement is met with $N/M \approx 1087$. The RTD Shannon entropies are similar, that is in agreement with the observed similar distributions in the histogram. The high rotational velocity simulation (2) shows a bit lower RTD Shannon entropy. This suggests a worse axial distributive mixing. This is also in agreement with the bit narrower distribution shown in the histogram.

All the simulations show a very similar RTD. The high rotational screw velocity simulation is a bit worse in axial distributive mixing compared to the other simulations.

In conclusion the RTD Shannon entropy is a suitable method for comparing axial mix quality.

7.5 Dispersive mixing, maximum shear stress results

Tracer particles were used to determine the maximum shear stress for flow paths within the spiral Maddock simulations. The shear stress due the simple shear flow in the gap between the barrier flight and the barrel is calculated with equation 18. Figure 40 shows both the maximum shear stress of the tracer particles and the analytically calculated shear stress in the gap.

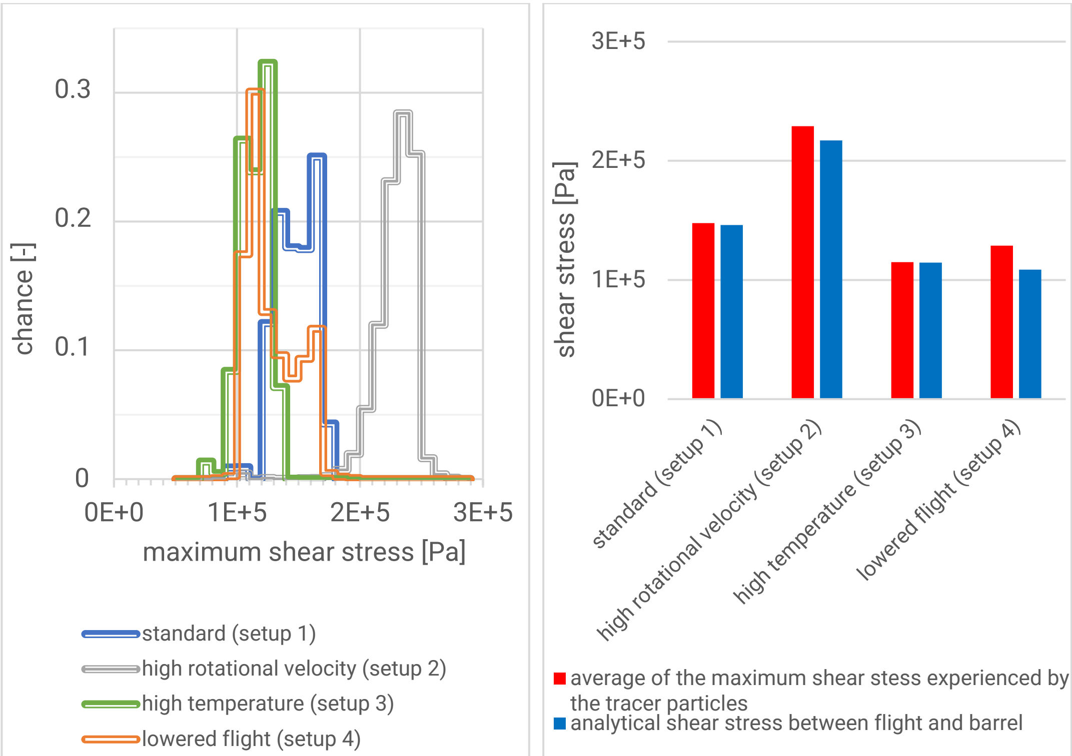

Figure 40. Left: a histogram of the maximum shear stress of the tracer particles. The bin size is 10^4 Pa. Right: the average of the maximum shear stress of the tracer particles and the analytical calculated shear stress due the simple shear flow between the barrier flight and the barrel.

The analytically calculated shear stress in the gap is very similar to the average of the maximum shear stress in the simulation. The average of the maximum shear stress is a bit higher than the analytically calculated shear stress in the gap. This suggests that numerous particles experience shear stress exceeding that caused solely by the simple shear flow in the gap. This could result from the pressure flow in the gap, which is incorporated in the simulation but not in the analytical calculations.

The distribution of maximum shear stress exhibited by tracer particles is attributed to the pressure flow in the gap. Furthermore, there is some scatter expected due to discretization in the simulation. This might reduce if a finer mesh is used.

The simulation with high screw rotational velocity, exhibiting the highest shear stresses, is therefore deemed the most effective dispersive mixer. The standard simulation is the second best dispersive mixer, but there is some overlap with the lowered flight simulation and the high temperature simulation.

In conclusion the maximum shear stress can be used to make a clear distinction in dispersive mix quality between several extrusion simulations.

8 Conclusion

Several methods, utilizing tracer particles, were developed to quantify mix quality in extrusion simulations. These methods demonstrated their effectiveness in a testing which involved comparisons of simulations across 4 variations of a spiral Maddock, each with different geometry, screw rotational velocity, and polymer temperature.

The mix quantification methods fall into two main categories: distributive mixing, which operates in three different dimensions, and dispersive mixing.

Angular and radial Shannon entropy

Some studies used Shannon entropy to determine mix quality over the cross section of an extruder, where higher values indicate a high mix quality, and lower values denote the opposite.

In the current study, the Shannon entropy is used as a key tool to understand the details of distributive mixing in extruder systems. The process requires dividing the extruder's outflow surface into bins, and using tracer particles introduced at the inflow to calculate the entropy. Depending on the specific requirements of the mixture, various bin distribution schemes can be employed to evaluate the mixing quality at different scales of observation or directions, including angular, radial, or two-dimensional.

The likelihood for random and systematic errors increases under conditions such as a low number of particles, a high number of bins, or a particle inflow section that surpasses the size of a single bin.

Changes in the extruder's variables notably influence the mix quality. For instance, an increase in the screw's rotational velocity enhances the angular distributive mixing quality leading to a higher angular Shannon entropy. On the other hand, a reduction in the height of the barrier flight improves radial distributive mixing quality causing an increase in radial Shannon entropy. However, neither temperature nor height of the barrier flight strongly influences the angular mix quality, and likewise, temperature and screw rotational velocity do not substantially affect the radial mix quality.

The positioning of the inflow particles also demonstrated a varying degree of influence on mixing quality.

Residence time distribution

In numerous studies, the Residence time distribution (RTD) serves as a measure of distributive mix quality in the axial direction, in both simulations and experiments. In this particular study, the RTD was quantified with the Shannon entropy. This method proved suitable to determine which is the better axial mixer. Out of the four compared mixers, the spiral Maddock with the standard geometry demonstrated the highest mix quality. Conversely, the simulations conducted with a higher rotational velocity and a lowered flight showed a reduced axial mix quality.

Dispersive mixing

Numerous studies have shown that particles, such as carbon black agglomerates, break-up at a critical shear stress. The link to shear stress was used, in the current study, to quantify dispersive mix quality in extrusion simulations. This method is very suitable for comparing mixers to each other. Out of the four compared mixers, the spiral Maddock with the high rotational velocity is the best dispersive mixer.

9 Recommendations

The simulation of sections from a single screw extruder was undertaken, and the mix quality was determined. It is recommended to verify simulated mixing quality with extrusion experiments in future research. Section 2 discusses several methods to determine mixing quality with extrusion experiments, as identified in the literature search. The most promising methods use RTD, Shannon entropy, optical methods and screw pulling.

In this study, the quality of dispersive mixing is characterized by shear stress within the extrusion simulation. While this method was effective for mixer comparison within simulations, it presented challenges when trying to compare with experimental results, given the inherent difficulty in measuring shear stress in an extruder. For dispersive mixing, experimental methods primarily concentrate on parameters like particle size and the increase in particle numbers. There is a clear need to either seek or develop a method that can calculate particle breakup in the extruder, allowing a direct comparison between the particle size and number in both experiments and simulations.

While the current study involved isothermal extrusion simulations, a certain degree of temperature increase should be anticipated, especially in dispersive mixing due to high shear stress. Investigating the temperature effects in non-isothermal simulations could provide valuable insights.

10 Acknowledgements

This study was financially supported by Tech For Future (TFF). The study was conducted by Windesheim University Professorship for Polymer Engineering. Wavin T&I provided HDPE, a capillary rheometer for rheological measurements and a single screw extruder for extrusion experiments. Furthermore, Wavin T&I provided notable feedback on this study and knowledge of the extrusion process.

References

1. Wang, W. and I. Zloczower. *Dispersive and distributive mixing characterization in extrusion equipment*. in *Antec 2001 Conference Proceedings*. 2001.
2. Tadmor, Z. and C.G. Gogos, *Principles of Polymer Processing*. 2006: Wiley.
3. Zhang, X.M., et al., *Assessing local residence time distributions in screw extruders through a new in-line measurement instrument.* Polymer Engineering & Science, 2006. **46**(4): p. 510-519.
4. Zhang, X.M., et al., *Local residence time, residence revolution, and residence volume distributions in twin-screw extruders.* Polymer Engineering & Science, 2008. **48**(1): p. 19-28.
5. Zhang, X.M., et al., *Numerical simulation and experimental validation of mixing performance of kneading discs in a twin screw extruder.* Polymer Engineering & Science, 2009. **49**(9): p. 1772-1783.
6. Zong, Y., H. Tang, and L. Zhao, *3-D numerical simulations for polycondensation of poly(p-phenylene terephthalamide) in twin screw extruder.* Polymer Engineering and Science, 2017. **57**(11): p. 1252-1261.
7. Tang, H., Y. Zong, and L. Zhao, *Numerical simulation of micromixing effect on the reactive flow in a co-rotating twin screw extruder.* Chinese Journal of Chemical Engineering, 2016. **24**(9): p. 1135-1146.
8. Xu, B., et al., *Evaluation of Mixing Performance in Baffled Screw Channel Using Lagrangian Particle Calculations.* Advances in Polymer Technology, 2017. **36**(1): p. 86-97.
9. Yamada, S., et al., *Dispersive mixing performance evaluation of special rotor segments in an intermeshing co-rotating twin-screw extruder by using weighted probability distributions.* International Polymer Processing, 2015. **30**(4): p. 451-459.
10. Chen, J. and Y. Cao. *Simulation of 3D flow field of RPVC in twin-screw extrusion under wall slip conditions*. in *Proceedings of 2012 9th International Bhurban Conference on Applied Sciences and Technology, IBCAST 2012*. 2012.
11. Equal to 3 and 6.
12. Manas-Zloczower, I., et al., *Color Mixing in Extrusion: Simulations and Experimental Validation*, in *NSF DMII Grantees Conference*. 2005: Scottsdale Arizona, USA.
13. Wang, W., I. Manas-Zloczower, and M. Kaufman, *Characterization of distributive mixing in polymer processing equipment using Renyi entropies.* International Polymer Processing, 2001. **16**(4): p. 315-322.
14. Wang, W., I. Manas-Zloczower, and M. Kaufman, *Entropic characterization of distributive mixing in polymer processing equipment.* AIChE Journal, 2003. **49**(7): p. 1637-1644.
15. Manas-Zloczower, I. and J.F. Agassant, *Mixing and Compounding of Polymers: Theory and Practice*. 2009: Hanser.
16. Alemaskin, K., et al. *Entropic mixing characterization in a single screw extruder*. in *SPE ANTEC*. 2004.
17. Alemaskin, K., et al. *Entropic measures of mixing tailored for various applications*. in *AIP Conference Proceedings*. 2004. AIP.
18. Alemaskin, K., I. Manas–Zloczowe, and M. Kaufman, *Index for simultaneous dispersive and distributive mixing characterization in processing equipment.* International Polymer Processing, 2004. **19**(4): p. 327-334.
19. Alemaskin, K., I. Manas-Zloczower, and M. Kaufman, *Entropic analysis of color homogeneity*. Polymer Engineering & Science, 2005. **45**(7): p. 1031-1038.
20. Alemaskin, K., I. Manas-Zloczower, and M. Kaufman, *Color mixing in the metering zone of a single screw extruder: numerical simulations and experimental validation.* Polymer Engineering & Science, 2005. **45**(7): p. 1011-1020.
21. Alemaskin, K., *Entropic Measures of Mixing in Application to Polymer Processing*. 2004, Case Western Reserve University.
22. Alemaskin, K., I. Manas-Zloczower, and M. Kaufman. *Simultaneous characterization of dispersive and distributive mixing in a single screw extruder*. in *Proceedings of the Int. Conf. ANTEC*. 2003.
23. Kutz, M., *Applied plastics engineering handbook: processing and materials*. 2011: William Andrew.

24. Mutagahywa, B.M., *Carbon black dispersion in rubber assessment methods and process studies*. 1984, © Beta Mutagwaba Mutagahywa.
25. Yamada, S., et al., *Analytical and Experimental Evaluation of Dispersive Mixing Performance of Special Rotor Segments in a Corotating Twin-Screw Extruder*. Polymer - Plastics Technology and Engineering, 2016. **55**(15): p. 1577-1585.
26. Hopmann, C., et al., *Analysis of mixing behavior of pin barrel extruders by means of simulative and experimental methods.* KGK Kautschuk Gummi Kunststoffe, 2016. **69**(5): p. 30-36.
27. MonTech, *MonTech Disper Tester 3000*.
28. Beetsma, J. *Optical properties of coating pigments: Absorption and scattering*. 2017 2017-2-10; Available from: https://knowledge.ulprospector.com/5871/pc-pigment-optical-properties-absorption-scattering/.
29. Chemloul, N.S., K. Chaib, and K. Mostefa, *Application of Pulsed Ultrasonic Doppler Velocimetry to the Simultaneous Measurement of Velocity and Concentration Profiles in Two Phase Flow*, in *Ultrasonic Waves*. 2012, InTech.
30. Takeda, Y., *Ultrasonic doppler velocity profiler for fluid flow*. 2012, Springer: Tokyo ;.
31. Petit, P., B. Birkhofer, and D. Lootens, *Wall shear measurement based on ultrasonic velocimetry for process inline rheometry.* 2010.
32. Putz, V., et al., *Adaptation of in-line ultrasonic velocimetry to melt flow measurement in polymer extrusion.* Measurement Science and Technology, 2013. **24**(10): p. 107002.
33. Putz, V., et al., *In–line ultrasonic melt flow measurement of polypropylene with different fillers.* Procedia Engineering, 2014. **87**: p. 156-159.
34. Dogan, N., M.J. McCarthy, and R.L. Powell, *Measurement of polymer melt rheology using ultrasonics-based in-line rheometry.* Measurement Science and Technology, 2005. **16**(8): p. 1684.
35. Ein-Mozaffari, F. and S.R. Upreti, *Using ultrasonic Doppler velocimetry and CFD modeling to investigate the mixing of non-Newtonian fluids possessing yield stress.* Chemical Engineering Research and Design, 2009. **87**(4): p. 515-523.
36. Kadlčák, J. and f. Univerzita Tomáše Bati ve Zlíně. Technologická, *Filler dispersion and rheology of polymers = Disperze plniv a reologie polymerů : doctoral thesis summary*. 2014, Tomas Bata University in Zlín: Zlín :.
37. BIPM, I., et al., *Evaluation of measurement data—guide for the expression of uncertainty in measurement. JCGM 100: 2008.* Citado en las, 2008: p. 167.
38. DIN, E., *ISO/IEC 17025 "General requirements for the competence of testing and calibration laboratories"*. 2017, April.
39. Buist, J., et al., *Polymer Mixing in a Single Screw Extruder (Part I: Simulation Method).* Windesheim, LKT-DP-106741-2212, 2022.

Professorship for Polymer Engineering

Polymer Mixing in a Single Screw Extruder

Part II: Mixing Quantification

About this Professorship

The Professorship for Polymer Engineering of University of Applied Sciences Windesheim was founded in 2009; the group's objective is to improve the knowledge base on sustainable processing of plastics and composites within and through the higher education system. Its primary function is as a research group in Polymer Engineering, delivering output in the field of applied science. The team operates within market based projects and comprises lecturers from Civil Engineering, Industrial Product Design and Mechanical Engineering. The output of the projects is integrated into the curriculum of these study programs.

Summary

In this TechForFuture project 'Polymer Mixing in a Single Screw Extruder' a method to optimize mixing elements is developed based on numerical simulations (Computational Fluid Dynamics, CFD). A numerical procedure is developed to calculate the flow field in the extruder. By tracing particles in this field data is collected to determine distributive and dispersive mixing. Based on these data measuring values, the so called resident time distribution and Shannon entropy, have been used to quantity mixing. This way numerical values can be compared to experimental values such that the developed procedure could be validated with experiment on a single screw extruder on labscale with different mixing elements. In the end, this numerical procedure can be used to analyze, optimize and judge different mixing elements with respect to their performance. The work has been carried out in close collaboration with Wavin T&I.

University of Applied Sciences Windesheim